The missing arcs of the India-Asia collision

Alexis Licht, Guillaume Dupont-Nivet, Jan Westerweel, Zaw Win, Abel Guihou, Pierre Deschamps, Day Wa Aung

Gondwana Research 147 (2025) 260–275

Contents lists available at ScienceDirect

Gondwana Research

journal homepage: www.elsevier.com/locate/gr

The missing arcs of the India-Asia collision

Alexis Licht [a,*], Guillaume Dupont-Nivet [b,c], Jan Westerweel [b], Zaw Win [d], Abel Guihou [a], Pierre Deschamps [a], Day Wa Aung [e]

[a] Aix-Marseille Université, CNRS, IRD, INRAE, CEREGE, Aix-en-Provence, France
[b] Géosciences Rennes, UMR CNRS 6118, Univ. Rennes, 35042 Rennes Cedex, France
[c] Potsdam University, Institute of Earth and Environmental Science, 14476 Potsdam, Germany
[d] Geology Department, Shwe Bo University, Sagaing Region, Myanmar
[e] Geology Department, Yangon University, Yangon Region, Myanmar

ARTICLE INFO

Handling Editor: Yunpeng Dong

Keywords:
Burma Terrane
India-Asia Collision
Trans-Tethyan Arc
Sedimentary provenance
Zircon

ABSTRACT

Sedimentary provenance studies indicate a Paleocene age for the India-Asia collision, based on the arrival of allochthonous sediment onto the Indian shelf. To account for this age, geodynamic models propose either an extra-large pre-collisional India or an initial collision between India and a Trans-Tethyan Arc situated offshore of Asia. The Burma Terrane is one of the proposed remnants of this arc. However, the existence of this arc has not been thoroughly investigated in regional sedimentary records. We gathered a large dataset (n > 40,000) of detrital zircon ages, including new and previously published data from eastern India, the Burma Terrane, and the Asian margin to identify age populations that could indicate the presence of this arc. Our synthesis suggests that the arrival of allochthonous material onto India is best explained by input from the Asian forearc (specifically, the Xigaze Forearc) alone, without requiring input from an additional missing arc. These constraints are compatible with Trans-Tethyan models only if they incorporate the Xigaze Forearc into the Trans-Tethyan Arc. Additionally, we show that the Burmese sedimentary record necessitates a missing Cretaceous-Paleogene arc located between Myanmar and Asia. Including the Burma Terrane and its missing arc in the Trans-Tethyan Arc is consistent with provenance and paleomagnetic data but implies a complex assembly history for the arc. Ultimately, a Trans-Tethyan Arc is not required to explain the history of the Burma Terrane and its detrital zircon record. Kinematic models involving an extra-large India and a Burma Terrane located offshore of Asia during the Paleogene are also compatible with these constraints.

1. Introduction

The modern structure and topography of the Tibetan-Himalayan orogen have been significantly shaped by the India-Asia collision, making the orogen a natural laboratory for studying continent–continent collisional systems (DeCelles et al., 1998; Kapp and DeCelles, 2019). However, the paleogeography of the India-Asia collision remains a debated issue. Sedimentary provenance studies, tracking the first input of allochthonous, Asia-derived sediment onto the Indian passive margin, provide a minimum Paleocene (ca. 61–59 Ma) age for the collision (Wu et al., 2014; Hu et al., 2015). Paleomagnetic constraints place the Indian continent at near-equatorial latitude at that time, thousands of kilometers away from the Asian margin (van Hinsbergen et al., 2011). To resolve this discrepancy, two widely different families of geodynamic models have been proposed.

The first family of geodynamic models proposes the existence of an extra-large Greater India, with over 2000 km of its northern tip having disappeared through subduction following the collision. This family exists in two versions: (a) a Greater India composed of continental crust (Ingalls et al., 2016), which requires continental subduction and significant shortening of the Asian margin to accommodate post-collisional convergence (Fig. 1a); (b) a large oceanic basin existing between modern continental India and the Himalayas (Fig. 1b). In this scenario, after the initial collision between the Himalayas and Asia in the Paleocene, this oceanic basin would have been subducted and closed until a subsequent, second collision between continental India and the Himalayas-Asia assemblage (van Hinsbergen et al., 2012).

The second family of geodynamic models proposes the existence of a Trans-Tethyan island arc that collided with the Indian continent in the Paleocene, and then, together, collided with Asia later in the Paleogene (Fig. 1c). Several terranes and magmatic arcs found around the India-Asia suture zone (the Indus-Tsangpo Suture Zone) have been

* Corresponding author.

https://doi.org/10.1016/j.gr.2025.06.018
Received 22 January 2025; Received in revised form 17 June 2025; Accepted 21 June 2025
Available online 11 July 2025

attributed to this Trans-Tethyan Arc: the Kohistan Arc in western Tibet (Jagoutz et al., 2015, 2019), the Burma Terrane southeast of the Eastern Himalayan Syntaxis (Westerweel et al., 2019), and isolated volcanic rocks along the suture (Spong and Dras arcs; e.g., Andjić et al., 2022). The forearc basin of the Lhasa Terrane in south-central Tibet, known as the Xigaze Forearc, has also been proposed to be part of the Trans-Tethyan Arc, as a fragment separated by back-arc rifting from the Asian margin (Xigaze Arc; Kapp and DeCelles, 2019; Xu et al., 2025). Multiple origin stories for the Trans-Tethyan Arc are currently debated, including a late Jurassic to mid-Cretaceous intra-oceanic origin (Jagoutz et al., 2019; Westerweel et al., 2024) or a back-arc rifting origin starting during the Jurassic (Zahirovic et al., 2016) or the late Cretaceous (Kapp and DeCelles, 2019).

Recent paleomagnetic data from the Burma Terrane of Myanmar (Westerweel et al., 2019) indicate that Burma Terrane rocks were located away from the Asian margin before the collision, during the mid-Cretaceous (ca. 100 Ma). These data support the Trans-Tethyan model and suggest a late Jurassic or early Cretaceous origin for the arc (Fig. 1c). This model posits that the initial Paleocene input of allochthonous material on the Indian passive margin reflects a collision with the Trans-Tethyan Arc rather than with the Asian margin.

In contrast, the recent kinematic model by Advokaat and van Hinsbergen (2024) reconciles the paleo-position of Myanmar with the extra-large Greater India model by suggesting that Myanmar was an isolated terrane offshore Sumatra before the collision, as a remnant of an earlier and wider Argoland archipelago (Fig. 1a & b). This model proposes that the Paleocene input of allochthonous material on the Indian passive margin reflects a collision of India with the Lhasa Terrane of the Asian margin, with a later Eocene collision between mainland India and Myanmar. The first input of Burma Terrane-derived rocks onto the Indian shelf is suggested to have occurred during the middle Eocene (Ding et al., 2022). However, the timing of this later collision has not been extensively addressed by source-to-sink approaches.

Sedimentary provenance studies using U-Pb ages of detrital zircons have played a critical role in identifying and dating the first input of allochthonous material on the Indian passive margin and subsequent regional changes in drainage related to the growth of the Tibetan-Himalayan orogen (Wu et al., 2014; Lang and Huntington, 2014; Bracciali et al., 2015; Hu et al., 2015). Asian terranes have experienced continuous magmatic activity since the Jurassic, which is absent on the Indian continent. Consequently, young (post-Triassic) zircon populations are attributed to Asian volcanic arcs and are used to identify Asia-derived sedimentary rocks (Hu et al., 2015; Baral et al., 2019; Ding et al., 2022).

However, distinguishing young zircons from the Asian subduction margin and from a hypothetical Trans-Tethyan island arc remains challenging, as both would have been active during the same time window (Jagoutz et al., 2019; Licht et al., 2020). Distinguishing an Indian, Trans-Tethyan, or Asian provenance with older (pre-Jurassic) zircon populations is also difficult because older zircons are often present in limited proportions compared to the overwhelming amount of younger, Cenozoic zircons. When present in large amounts, these older zircons often display similar age populations due to their shared Gondwanan origin and Protero-Paleozoic magmatic history (Gehrels et al., 2011). These challenges hinder the identification of zircon populations in sedimentary records that could be used to test the different geodynamic scenarios.

However, the proportion of each age population often varies among individual terranes (Gehrels et al., 2011; Licht et al., 2016a). These variations depend on the local tectono-magmatic history (e.g., varying intensity of magmatic flare-ups) and on the local history of sediment mixing and recycling (e.g., varying supply of sediment from distant areas that is later incorporated into local sediment through recycling; Licht et al., 2024). Identifying these regional variations and using them to track changes in provenance requires a significant amount of zircon ages per sample/per area ($n > 500$–800, depending on the number of individual age populations; Pullen et al., 2014).

In this paper, we provide new zircon U-Pb ages from Cretaceous and Cenozoic rocks of Myanmar, one of the proposed remnants of the hypothetical Trans-Tethyan Arc. We then utilize the statistical advantages of "large n" single mineral geochronology to test the geodynamic scenarios proposed for the India-Asia collision. We compile an extensive dataset ($n > 40{,}000$) of detrital zircons from Cretaceous and Cenozoic sedimentary rocks spanning the eastern edge of the India-Asia collision zone, where Indian, Burmese (Trans-Tethyan?), and Asian basins have been accreted. We leverage this dataset and employ statistical mixture modeling methods to identify the sedimentary contributions of individual terranes to these different basins and test their consistency with the various India-Asia collision models.

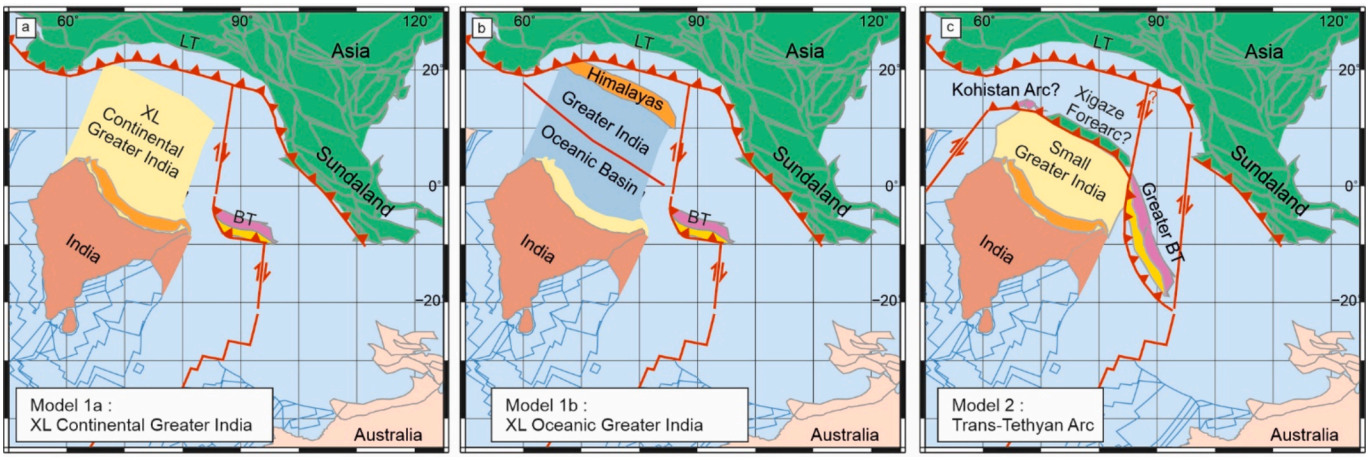

Fig. 1. Plate reconstruction at ca. 60 Ma highlighting the two families of geodynamic models for the India-Asia Collision with their variations (plate models after Westerweel et al., 2019; Advokaat and van Hinsbergen, 2024). (a) single collision with an extra-large (XL) Greater India made of continental crust (Ingalls et al., 2016); (b) single collision with an extra-large Greater India made of an oceanic basin separating the Himalayas from mainland India (van Hinsbergen et al., 2012); (c) dual collision including a first collision a Trans-Tethyan Arc including either the Burma Terrane (Westerweel et al., 2019) and/or the Kohistan Arc (Jagoutz et al., 2019) and/or the Xigaze Forearc (Kapp and DeCelles, 2019). BT: Burma Terrane; LT: Lhasa Terrane. Red lines indicate the main plate boundaries (subduction, transform zones and spreading ridges). The main geological provinces addressed in this study are highlighted with different colors: Asia (in green), Continental India (brown), the Himalayas (orange), the Burma Terrane (purple) and the Indo-Burman Ranges (dark yellow).

2. Geological context

This section describes the sedimentary basins investigated in light of their detrital zircon signatures, with a particular emphasis on Myanmar, where we present new detrital zircon data.

2.1. The Central Myanmar Basins (CMB) of the Burma Terrane

Western Myanmar is part of an individual terrane often referred to as the Burma Terrane. It is almost entirely covered by the Central Myanmar Basins (CMB), a north–south belt of Late Cretaceous to Cenozoic sedimentary basins separated into two lateral troughs of sub-basins by the Wuntho-Popa Magmatic Arc (WPA, Fig. 2a; Licht et al., 2020). The basement of the Burma Terrane includes the magmatic rocks of the WPA, as well as Paleozoic and Mesozoic metamorphic rocks that crop out in northern Myanmar (Jade Belt, Minwun Ranges, Tagaung-Myitkyina Belt, and Kumon Range; see Mitchell, 2017 for a detailed review). The Katha-Gangaw Range in northeastern Myanmar is composed of Triassic to Jurassic metasedimentary rocks and Jurassic to Cretaceous mafic plutons and has recently been proposed as the southern continuation of the Lhasa Terrane of Asia, based on the affinity of its detrital zircons (Min et al., 2022). The extent to which the northern part of the Burma Terrane (i.e., Greater Burma Terrane; Fig. 1c) was shortened, subducted, and underthrust in the Eastern Himalayan Syntaxis since the Paleogene remains unclear (Morley et al., 2020; Westerweel et al., 2020).

Paleomagnetic data from WPA plutons and CMB sedimentary rocks place the Burma Terrane near the equator in the early Cretaceous (ca. 100 Ma), distant from the Indian Plate to the south and the Asian margin to the north (Westerweel et al., 2019). Various age estimates for the collision between the Burma Terrane and Asia have been proposed based on structural and kinematic constraints, ranging from the Eocene to the Miocene (Westerweel et al., 2019; 2020; Morley et al., 2020; Advokaat and van Hinsbergen, 2024). The eastern margin of the Burma Terrane and its transition to the Sundaland part of Asia is marked by the metamorphic Mogok-Mandalay-Mergui Belt (MMMB, Fig. 2b). The MMMB has been interpreted as the western margin of the Sibumasu Terrane of Sundaland and has been gradually exhumed since the late Eocene (Mitchell, 2017).

The upper Cretaceous to Cenozoic stratigraphy of the CMB is displayed in Fig. 3a. The sequence begins with mid-Cretaceous shallow marine carbonates, followed by Campanian-Maastrichtian mudstones and carbonates. After an unconformity dated to the latest Cretaceous to earliest Paleocene, the Paleocene-Eocene sequence includes various geological units consisting of shallow marine siliciclastics with rare continental episodes (Licht et al., 2019; Cai et al., 2020). Two major unconformities are identified in the northern CMB, occurring in the late Eocene and latest Oligocene to early Miocene (Westerweel et al., 2020). Cenozoic rutile grains and zircons with negative εHf values, attributed to the MMMB, appear directly after the first unconformity in early Oligocene units of the CMB and are interpreted as the first marker of the collision between the Burma Terrane and Asia (Najman et al., 2022). Earlier units yield prominent Cretaceous to Cenozoic zircon ages, including three major peaks at 50, 70, and 95 Ma (Bandopadhyay et al., 2022). The late Cretaceous and early Eocene populations (70 and 50 Ma) are absent in Wuntho-Popa plutons, which have ages of 40 and 100 Ma only (Licht et al., 2020). The provenance of these populations were alternately attributed to a long-distance connection with poorly dated plutons in northern Myanmar, the Gangdese Arc of the Asian margin in Tibet (Robinson et al., 2014; Westerweel et al., 2020; 2024), or a missing part of the WPA located further east of the Burma Terrane that disappeared through subduction along the Asian margin in Sibumasu (Bandopadhyay et al., 2022).

Oligo-Miocene deposits are continental in the northern CMB and alternate between continental and shallow marine in the southern CMB (McNeil et al., 2021). Miocene deposits display numerous local unconformities related to the onset of a regional compressive regime in central Myanmar and local inversions of the CMB (Pivnik et al., 1998). Detrital zircons from Oligo-Miocene samples have been alternately used to argue for the establishment of modern river drainage in the early (Zhang et al., 2019) or late Miocene (Jonell et al., 2022).

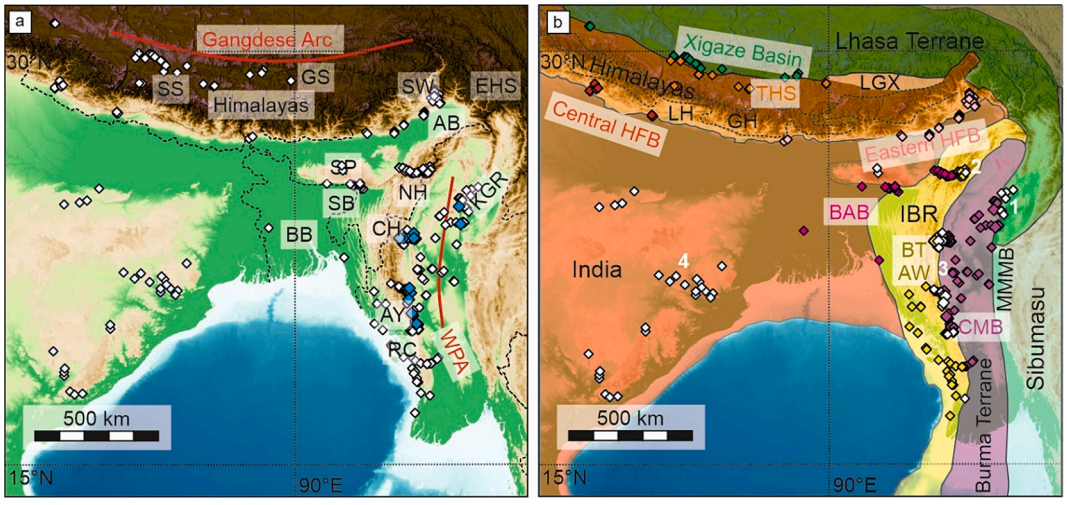

Fig. 2. (a) Eastern edge of the India-Asia collision zone; red lines indicate Cenozoic volcanic arcs; dashed lines are administrative borders. Diamonds are detrital zircons samples used in this study (white diamonds: previously published samples; blue diamonds: new samples). WPA: Wuntho-Popa Arc; KGR: Katha-Gangaw Range; EHS: Eastern Himalayan Syntaxis; AB: Assam Basin; SP: Shillong Plateau; SB: Surma Basin; BB: Bengal Basin; NH: Naga Hills; CH: Chin Hills; AY: Arakan Yoma; RC: Rakhine Coast; SW: Siang Window; SS: Sangdanlin Section; GS: Gyangze Section. **(b)** main terranes and structural units (terrane color coding similar to Fig. 1). Samples (diamonds) are colored according to their geological region (see main text): Central Myanmar Basins (CMB, in dark purple), Burma Terrane Accretionary Wedge (BTAW, in yellow), Bengal and Assam Basins (BAB, in light purple), central and eastern Himalayan Foreland Basin (HFB, in red –central HFB- and pink –eastern HFB-), Tethyan Himalayan Series (THS, in orange), Xigaze Basin (in green). White diamonds correspond to basement rock samples (1: Katha-Gangaw Range; 2: Naga Metamorphics; 3: Triassic-early Jurassic Pane Chaung Formation and Kanpetlet Schists; 4: Pre-Cretaceous continental India). LH: Lesser Himalayas; GH: Greater Himalaya (boundaries highlighted with dashed lines); LGX: Langjiexue fold & Trust belt in the THS (area highlighted in light orange); IBR: Indo-Burman Ranges; MMMB: Mogok-Mandalay-Mergui Belt.

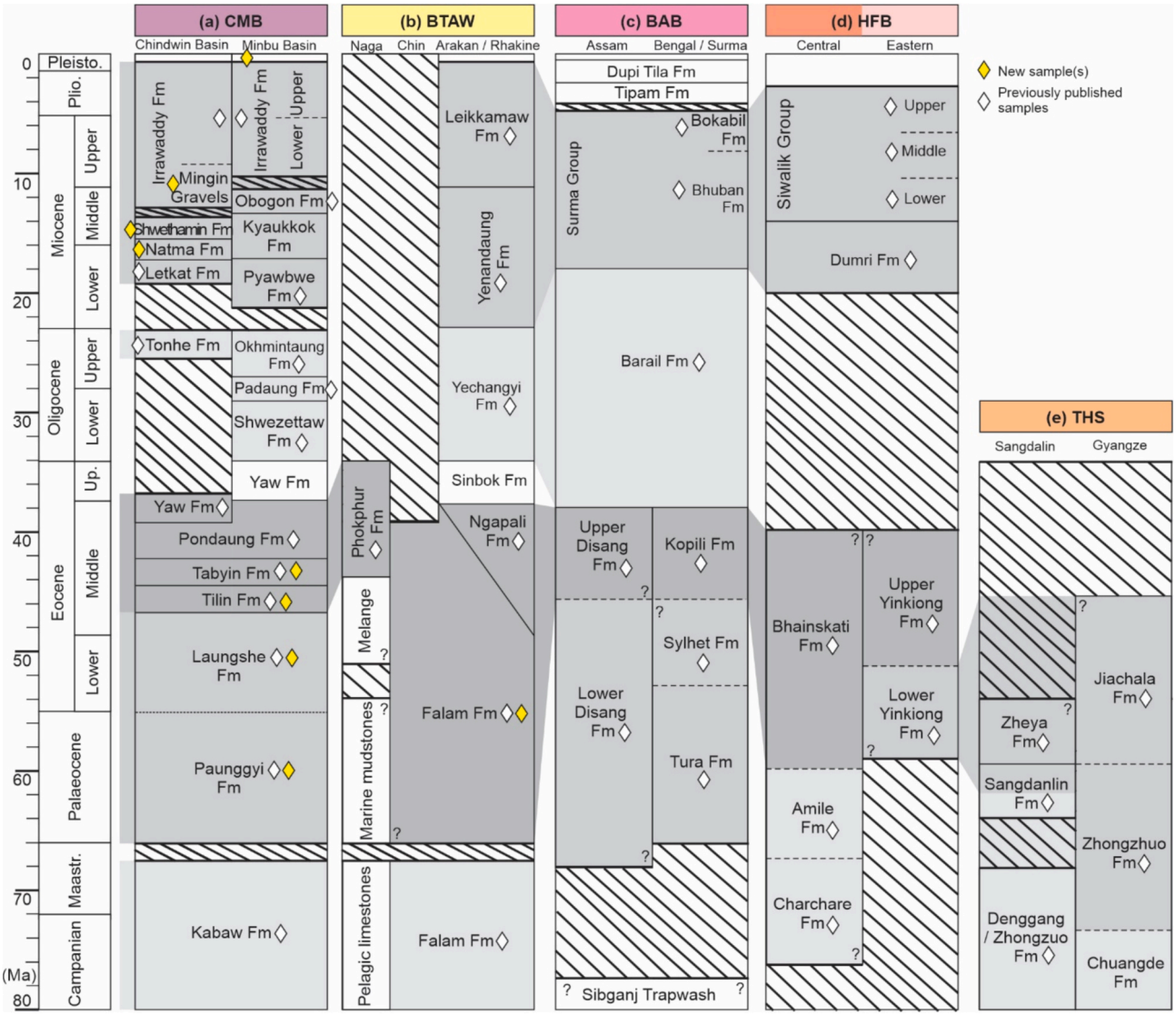

Fig. 3. Stratigraphy of the main basins at the eastern edge of the India-Asia collision zone, including (a) Central Myanmar Basins (CMB, in dark purple; two main basins are displayed: the Chindwin Basin of northern Myanmar, and the Minbu Basin of southern Myanmar; after Licht et al., 2019); (b) the Burma Terrane Accretionary Wedge (BTAW, in yellow; three main areas are displayed: the Naga Hills of northern Myanmar, Chin Hills of central Myanmar, and Arakan Yoma / Rhakine Coast of southern Myanmar; after Aitchison et al., 2019; Naing et al., 2014); (c) the Bengal and Assam Basins (BAB, in light purple; after Bracciali et al., 2015; Ding et al., 2022); (d) the Himalayan Foreland Basin (HFB, separated in a central and eastern segments, in orange and pink; after DeCelles et al., 2004; Baral et al., 2019), and (e) the Tethyan Himalayan Series (THS, in orange; two main areas are displayed: the Sangdanlin and the Gyangze sections; after DeCelles et al., 2014; Wu et al., 2014). The stratigraphic position of the samples used in the study is indicated by diamonds (white: previously published samples; yellow: new samples). Oblique lines indicate sedimentary gaps (and thus, unconformities). The time slice division of the age compilations from Figs. 4, 5 and 6 is highlighted with grey shades.

2.2. The Burma Terrane Accretionary wedge (BTAW) in the Indo-Burman Ranges

On its western margin, the Burma Terrane is separated from the Bay of Bengal and the Indian shelf by the Indo-Burman Ranges (IBR), which form the Burma Terrane Accretionary Wedge (BTAW) produced by the subduction of the Indian Plate beneath the Burmese active margin (Morley et al., 2020). The inner wedge of the IBR comprises Early Cretaceous ophiolites, the Paleozoic Naga Metamorphics, and Triassic-Early Jurassic metasedimentary rocks (Pane Chang Formation and Kanpetlet Schists; Naing et al., 2023). The Early Cretaceous ophiolites have been correlated with the Indus-Tsangpo Suture Zone ophiolites based on their age and geochemistry, while the metasedimentary units have been correlated with the Langjiexue Group of the Tethyan Himalayan Series (see section 2.5; Yao et al., 2017; Aitchison et al., 2019). These units have been part of the Burma Terrane basement since at least the Early Cretaceous, as the Pane Chaung Formation is overlain by the same mid-Cretaceous shallow marine carbonates found in the CMB (Morley et al., 2020). The Pane Chaung Formation and other pre-Cretaceous metasedimentary units in the IBR have been interpreted as once part of Argoland, a wide archipelago separated from Gondwana, and later accreted to the BTAW (Morley et al., 2020; Advokaat and Van Hinsbergen, 2024). Late Cretaceous to Cenozoic siliciclastic deposits overlie the mid-Cretaceous carbonates; their stratigraphy is summarized in Fig. 3b.

In the central (Chin Hills) and southern (Arakan Yoma and Rakhine Coast) segments of the IBR, Late Cretaceous to Eocene deposits are grouped under the Falam Formation, which possibly encompasses an unconformity near the Cretaceous-Paleogene boundary (Naing et al., 2023). The stratigraphy of the northern segment (Naga Hills) has been

less studied. There, the Eocene Phopkhur Formation overlies a lower-middle (?) Eocene ophiolitic mélange, the formation of which is attributed to the thrusting of the Early Cretaceous ophiolite onto the Indian passive margin (Aitchison et al., 2019).

In the northern and central segments of the IBR, sedimentation stopped in the inner wedge during the middle to late (?) Eocene. Low-temperature thermochronology indicates two episodes of exhumation in these segments, during the middle Eocene and latest Oligocene-early Miocene (Najman et al., 2022). In the southern IBR, where the inner wedge faces the Indian Ocean, sedimentation continued over the Oligocene and Miocene (Naing et al., 2014). All the deposits of the inner wedge have been interpreted as having been deposited along the Burma Terrane active margin in an accretionary wedge setting, sourced from the WPA and the Burma Terrane basement (Najman et al., 2020; Naing et al., 2023).

The IBR outer wedge consists of Neogene clastic sequences from the eastern Indian Foreland and its peripheral basins that were incorporated into the wedge during the late Neogene (Morley et al., 2020). In the northern segment of the IBR (Naga Hills), geological units from the outer wedge are indistinguishable from those of the Assam Basin of the eastern Indian Foreland Basin (see next subsection), and ophiolites and mélange units from the inner wedge are directly thrusted above them (Aitchison et al., 2019).

2.3. The Bengal and Assam basins (BAB)

We group under the name “Bengal and Assam Basins” (BAB) the Upper Cretaceous to Cenozoic deposits of the Assam Basin, Bengal Basin (including the Surma Basin, also known as the Sylhet Trough), and the units of the outer wedge of the northern segment of the IBR (Aitchison et al., 2019; Ding et al., 2022). These sedimentary rocks were deposited on the easternmost portion of the Indian shelf during the time window proposed for the collision(s) between India, Asia, the hypothetical Trans-Tethyan Arc, and the Burma Terrane. These regions were likely parts of the same basin system until the uplift of the Shillong Plateau in the late Miocene, which today separates these basins (Fig. 2a; Govin et al., 2018). The different parts of the BAB show an overall similar stratigraphic sequence (Fig. 3c).

This sequence unconformably overlies Lower Cretaceous volcaniclastics of the Indian shelf (Alam et al., 2003). These Lower Cretaceous volcaniclastics are sporadically found in northern India and are associated with an episode of intracontinental rifting that hypothetically separated the Himalayas from continental India (van Hinsbergen et al., 2012). Upper Cretaceous to middle Eocene units (Tura, Sylhet, and Kopili Formations in the south, Disang Formation in the north) are regionally shallow marine. They are followed by the upper Eocene to Oligocene Barail Group, marking the establishment of a wide, southward-prograding deltaic system (Najman et al., 2008). Zircon U-Pb and fission track ages, as well as Ar-Ar mica ages, Cr-spinel geochemistry, and sandstone petrography, suggest the arrival of Himalaya-derived sources within the Barail Group (Najman et al., 2008).

Cenozoic zircon ages in earlier units have been alternately used to argue for an early to middle Eocene drainage connection with the Gangdese Arc of the Asian margin in Tibet (Najman et al., 2008; Yang et al., 2019) or an input from the WPA of the Burma Terrane (Ding et al., 2022). The later, Mio-Pliocene units (Surma, Tipam, and Dupi-Tila Groups) are prominently deltaic in the Bengal Basin and fluvial in Assam. Their detrital zircons, rutile grains, and sandstone petrography indicate a persistent Himalaya-derived source and Transhimalayan arc signature, suggesting the establishment of the modern Yarlung–Siang–Brahmaputra river system in the early Miocene (Bracciali et al., 2015; Vadlamani et al., 2015; Rahman et al., 2017).

2.4. The Himalayan foreland Basin (HFB)

We group under the name “Himalayan Foreland Basin” (HFB) the Upper Cretaceous to Cenozoic geological units found in the Lesser Himalayas and Sub-Himalayan Zone of the Tibetan-Himalayan orogen (DeCelles et al., 1998). These units include (Fig. 3d): the Upper Cretaceous to Miocene deposits of the Lesser Himalayas in Nepal and India (Feng et al., 2023), the Paleogene deposits of the Siang window in the eastern Himalayan Syntaxis (Baral et al., 2019), and the Mio-Pliocene Siwalik Group in the Sub-Himalayan zone (Lang and Huntington, 2014). All these units were deposited on the Indian shelf facing the collision front with the Lhasa Terrane of continental Asia.

In the central segment of the HFB, the Lesser Himalayas sequence unconformably overlies Paleozoic basement rocks of the Indian Shelf (Gehrels et al., 2011). It begins with Cretaceous volcaniclastics (Amile and Taltung Formations), which are unconformably overlain by lower to middle Eocene siliciclastic deposits (Bhainskati or Subathu Formation; DeCelles et al., 1998). Variations in detrital zircon populations between Cretaceous and Eocene units have been used to argue for the onset of erosion of Tethyan Himalayan rocks in the nascent Himalayan thrust belt during the early Eocene (DeCelles et al., 2004; Feng et al., 2023). The Eocene units are unconformably overlain by the lower Miocene Dumri Formation, which extends further south into the Sub-Himalayan zone and records the onset of input from the metamorphosed Greater Himalayan zone (DeCelles et al., 2004; Feng et al., 2023).

In the eastern segment of the HFB, Paleogene deposits consist exclusively of the late Paleocene to middle Eocene Yinkiong Formation found in the Siang window (Acharyya, 2007). This formation is folded and thrust with the lower Cretaceous Abor Volcanics, associated with an early Cretaceous episode of intra-continental rifting (Baral et al., 2022). Changes in detrital zircon populations between the lower and upper members of the Yinkiong Formation (including the appearance of Cenozoic ages) suggest an input of Asia-derived sediment in the early Eocene, marking the onset of the India-Asia collision (Baral et al., 2019).

The Mio-Pliocene Siwalik Group is widespread south of the Himalayas in the Sub-Himalayan zone and is present in both the central and eastern segments. Sedimentary provenance studies indicate a direct, proximal provenance from the Himalayas, including Lesser, Greater, and Tethyan Himalayan units (Ravikant et al., 2011). In the eastern part of the Sub-Himalayan zone (Assam), where the northern and eastern Indian foreland basins overlap, the Siwalik Group contains Cenozoic zircons attributed to the Gangdese Arc of Tibet, suggesting the establishment of the Yarlung–Siang–Brahmaputra River in the early Neogene (Lang and Huntington, 2014).

2.5. The Tethyan Himalayan Series (THS) and the northern tip of India

The Tethyan Himalayan Series (THS) represents the northernmost unit of the Himalayas, consisting of Neoproterozoic to Paleogene clastic deposits of Indian affinity (Gehrels et al., 2011). Since the Triassic, when the Lhasa Terrane separated from India, the THS units have been deposited along the northern edge of the Greater India passive margin (Garzanti and Hu, 2015). In the easternmost segment of the THS, deposits from the Langjiexue fold and thrust belt, including the Triassic Langjiexue Group, feature a significant 280–210 Ma zircon population that is notably absent elsewhere in the THS (Liu et al., 2020). This age population may reflect a local source, either from the rifting Lhasa Terrane (Liu et al., 2020) or the distant Papua Arc (Yao et al., 2017). The age distribution of this population is very similar to that of the Triassic to lower Jurassic metasedimentary basement of the Indo-Burman Ranges (IBR), suggesting a comparable geographical origin (Yao et al., 2017; Liu et al., 2020).

Upper Cretaceous to middle Eocene units of the THS exhibit a gradual transition from upper slope to shelf and eventually to fluviatile environments (Hu et al., 2012). These units are exposed in various locations, including the Sangdanlin and Gyangze areas, where their provenance has been extensively studied (Fig. 2a and 3e). Detrital zircons from Upper Cretaceous and Paleocene rocks indicate significant recycling from earlier Tethyan Himalayan units, suggesting deposition

in local turbidite fans along the slope of Greater India (DeCelles et al., 2014). Cenozoic detrital zircons first appear in late Paleocene sediment (ca. 61–59 Ma) at the Sangdanlin section, marking the initial input of Asia-derived sediment from the Gangdese Arc onto the Indian shelf (Hu et al., 2015). Cenozoic zircons are also found at the base of the Zhongzuo Formation in the Gyangze area, although the age of this formation, spanning late Cretaceous to Paleocene, is less precisely constrained (Wu et al., 2014). Subsequent late Paleocene to middle Eocene units are interpreted as representing the most proximal, foredeep zone of the northern Indian foreland basin. The cessation of sedimentation in the middle Eocene is viewed as signifying the migration of the foredeep toward the Lesser Himalayas and the Sub-Himalayan zone (DeCelles et al., 2014).

2.6. The Xigaze Basin and the Asian forearc

The Xigaze Basin, located directly south of the Gangdese Arc of the Lhasa Terrane in Tibet, served as the forearc basin for subduction along the Asian margin prior to India's collision with Asia (Kapp and DeCelles, 2019). Its basement consists of early Cretaceous ophiolites from the Indus-Tsangpo Suture Zone ophiolitic belt, with sedimentation commencing shortly after the ophiolitic spreading in the mid-Cretaceous and continuing until the early Eocene (Orme et al., 2015; Wang et al., 2017). The sediments in the Xigaze Basin are interpreted as being primarily sourced from the Gangdese Arc and the Lhasa Terrane basement (Aitchison et al., 2011; Orme et al., 2015). Detrital zircon data from the Xigaze Basin, along with the Tethyan Himalayan Series (THS), indicate that the Xigaze Forearc was a major source of Asia-derived sediment reaching the Indian shelf after the late Paleocene (Orme et al., 2015). However, it remains uncertain whether the Xigaze Forearc was positioned directly south of the Gangdese Arc or located hundreds of kilometers offshore from the Asian margin, potentially as part of a Trans-Tethyan Arc at the time of the collision (Kapp and DeCelles, 2019).

3. Samples and methods

3.1. U-pb dating of detrital zircons from Myanmar

Between 2017 and 2020, we sampled various geological units from the Central Myanmar Basins (CMB) and the Indo-Burma Ranges of Myanmar for U-Pb dating of detrital zircons. The complete list of samples, including their origin and exact locations, is provided in Supplementary Table 1. We collected 2–3 kg of sandstones from the field for each sample, separated zircon grains using standard heavy liquid techniques, and mounted them in epoxy resin. Laser spots for ablation were selected randomly ("blind-dating" approach), and the selected zircon grains were dated by laser ablation inductively coupled plasma mass spectrometry (LA-ICP-MS).

Twenty-two samples were analyzed at the University of Washington, using an iCAP-RQ Quadrupole ICP-MS coupled to an Analyte G2 excimer laser. Zircons were ablated with a spot diameter of 25 μm, a 10 Hz pulse repetition rate, an energy fluence of 4.12 J/cm^2, and a carrier gas flow of 0.65 L/min. Data reduction, date, and date uncertainty calculations were performed using Iolite (Version 3.5) and an in-house MATLAB script. Details about our U-Pb dating workflow, data reduction steps, and discordance filters are provided in Shekut and Licht (2020). The ten zircon validation reference materials used during these sessions yielded offsets around TIMS ages < 1 % in most cases, and < 2 % otherwise.

Five additional samples were analyzed at the Envitop analytical facility at CEREGE (Centre for Research and Education in Environmental Geosciences) using an Element XR ICP-MS connected to a NWR193 laser (ArF 193 nm) ablation system. Zircons were ablated with a 25 μm spot diameter, a 15 Hz pulse repetition rate, an energy fluence of 1.5 J/cm^2, and a carrier gas flow of 0.975 L/min. Data reduction, date, and date uncertainty calculations were conducted with an in-house MATLAB script. The discordance filter used to screen for concordant grains is the Concordia distance of Vermeesch (2021) using isometric logratios and a threshold of 10 (SI) for discordance and 5 (SI) for reverse discordance. Details about our U-Pb dating workflow, data reduction steps, and discordance filter are given in Licht et al. (2024). The three zircon validation reference materials used during these sessions yielded offsets around TIMS ages < 1 % in most cases, and < 2 % otherwise.

In total, our dataset includes 7,886 concordant new ages. Detailed data are available in Supplementary Table 1.

3.2. Data compilation

We compiled a comprehensive dataset of concordant detrital zircon ages from Cretaceous and Cenozoic sedimentary rocks across the eastern edge of the India-Asia collision zone, as well as potential source rocks. This dataset includes 44,569 ages from 496 samples, derived from 57 published studies. Due to the variability in data reporting standards, especially in studies conducted before 2015, we did not apply a uniform filter for concordance but used the ages identified as concordant by each individual study. This approach addresses the inconsistency in data reporting and concordance calculation methods (Horstwood et al., 2016; Vermeesch, 2021). The list of all samples and their references is provided in Supplementary Table 2.

The source rock compilations are displayed in Fig. 4 and include:

- Cretaceous and Paleogene sedimentary rocks from the Xigaze Basin of the Lhasa Terrane.
- Pre-Cretaceous rocks from the Katha-Gangaw Range of northern Myanmar.
- Paleozoic Naga Metamorphics in the inner wedge of the IBR (Naga Hills).
- Triassic-lower Jurassic rocks in the inner wedge of the IBR (Pane Chaung and Kanpetlet Formations in the Chin Hills and Arakan Yoma).
- The Triassic Langjiexue Group of the eastern THS (compilation from Liu et al., 2020).
- Pre-Cretaceous rocks from continental India (excluding the Himalayas; compilation extracted from Puetz and Condie, 2019).

The sedimentary rock compilations include:

- The Central Myanmar Basins (CMB) (Fig. 5a).
- The Burma Terrane Accretionary Wedge (BTAW) (Fig. 5b).
- The Bengal and Assam Basins (BAB) (Fig. 5c).
- The Eastern segment of the Himalayan Foreland Basin (HFB) (Fig. 6a).
- The Central segment of the HFB (Fig. 6b).
- The Tethyan Himalayan Series (THS) (Fig. 6c).

The samples from the sedimentary rock compilations are divided into time slices based on the age of their geological units, as highlighted in Fig. 3. For the THS, the Cretaceous-lower Paleocene compilation includes samples dated before 61 Ma and identified as pre-collisional by Wu et al. (2014) and Hu et al. (2015), while the late Paleocene-Eocene compilation includes all subsequent samples. For the HFB, samples are divided into eastern and central segments, with an arbitrary cut-off longitude at 88°E (see Fig. 2).

3.3. Mixture modeling approach

To test the potential mixed contributions of different allochthonous sources in the upper Cretaceous-Cenozoic sedimentary basins, we employed the mixture algorithm developed by Licht et al. (2016a, b; 2024). This method involves modeling synthetic age distributions by randomly selecting ages from the source populations and comparing these synthetic distributions to the actual compiled age distributions from the sedimentary basins.

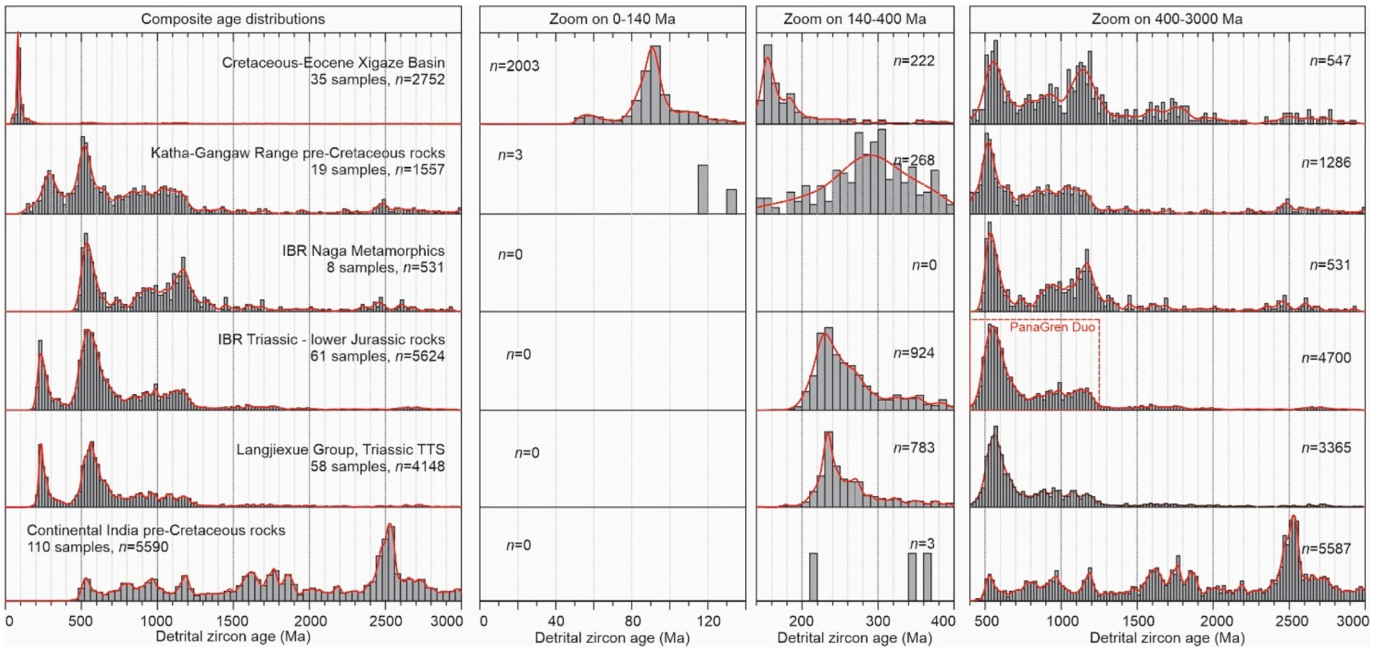

Fig. 4. Histograms and kernel density estimate diagrams for potential sediment source areas that are discussed in this study: The Xigaze Basin of the Lhasa Terrane, the Katha-Gangaw Range of northern Myanmar, the Naga metamorphics in the IBR Naga Hills, the IBR Triassic – lower Jurassic basement, The Langjiexue Group of the eastern THS, and pre-Cretaceous basement rocks of continental India. "PanaGren" refers to Panafrican (500–700 Ma) and Grenvillian (800–1300 Ma) zircon populations. Ages in histograms are displayed in 20 Ma bins (0 to 3000 Ma, 400 to 3000 Ma), 5 Ma bins (0 to 140 Ma), and 10 Ma bins (140 to 400 Ma). See Supplementary Text for the sample list and references of each age compilation.

For each possible combination of three different sources, we modeled N synthetic age distributions of 100 ages each (the average number of ages per sample in the zircon database). N was chosen to be large enough to capture the potential variability in age proportions created by zircon subsampling (N = 200; Licht et al., 2016a). We then calculated the average statistical dissimilarity between each of these N synthetic age distributions and the actual age distributions. The combinations yielding the lowest N-averaged dissimilarity values indicate the mixtures that best reproduce the zircon age distribution of the sedimentary basins.

We used the Kolmogorov-Smirnov (KS) statistic as the dissimilarity measure, a classical and widely-used indicator in detrital zircon studies (Licht et al., 2016b; 2024; Vermeesch, 2018). This mixture modeling approach is most effective when the zircon age compilations from both the sources and the sedimentary basins are large enough to increase the statistical significance of each age peak contribution. According to Licht et al. (2016a), compilations with more than 800 zircon ages allow the effective use of this approach with Asian terranes.

4. Results

Age distributions of the new samples from the CMB and the BTAW are shown in Supplementary Fig. SM1 and discussed in the supplementary text. This section focuses on the results from the regional age compilations.

4.1. Potential sources areas

The age distributions from the Xigaze Basin, Katha-Gangaw Range in northern Myanmar, Naga metamorphics, Triassic-Lower Jurassic strata in the IBR and the Langjiexue Group of the eastern THS display the same Precambrian-Cambrian ages, with a prominent Panafrican (500–700 Ma) population and a broader Grenvillian (800–1300 Ma) population (hereby referred to as the "PanaGren duo"; see Fig. 4). Two secondary populations, Eburnean (1600–1900 Ma) and Liberian (2400–2800 Ma), are found in Xigaze Basin rocks; they are almost absent in Katha-Gangaw and IBR rocks. All these populations are expressed in Pre-Cretaceous continental India, with a prominence of the older Eburnean and Liberian populations.

IBR Triassic-Lower Jurassic rocks and the THS Langjiexue Group display a clear Permian-Triassic (210–280 Ma) age population centered around ca. 230 Ma, while Katha-Gangaw rocks display a broader Carboniferous-Triassic (230–350 Ma) population centered around ca. 290 Ma. These populations are absent from the other source areas considered here. Xigaze Basin rocks display a continuous record of ages from the late Triassic to the Eocene, with two prominent populations centered around 155 Ma and 90 Ma, and a younger and smaller population centered at 60 Ma. Restricting the Xigaze Basin compilation to Paleocene-Eocene samples (18 samples) or Eocene samples (16 samples) results in a minor increase in the size of the 60 Ma population (not shown).

4.2. Central Myanmar Basins (CMB)

All age compilations from the CMB display a well-marked PanaGren duo and a Triassic age population similar in shape to that of the IBR Triassic-Jurassic rocks and the Langjiexue Group (Fig. 5a). These are overwhelmed by a continuous Upper Cretaceous-Cenozoic zircon population. Three age peaks can be distinguished, similar to those identified by Bandopadhyay et al. (2022): 95, 70, and 50 Ma. The 90 Ma population is prominent in Cretaceous to Middle Eocene compilations. The 50 Ma population appears in middle Eocene samples; it becomes prominent and widens to incorporate the 70 Ma population in the Miocene compilation.

We note a minor Jurassic (140–180 Ma) age population, similar to the one found in Xigaze rocks, that appears in the middle Eocene and becomes well-marked in the Oligocene and Miocene compilations. This population is almost absent in the Paleocene-lower Eocene compilation; the Cretaceous compilation does not have enough pre-Cretaceous ages to be conclusive about its presence.

Fig. 5. (a) Histograms and kernel density estimate diagrams for the age compilations from samples of the CMB, (b) the Burma Terrane Accretionary Wedge (BTAW) and (c) the Bengal and Assam Basins (BAB). Time slices shown on Fig. 3, color coding and legend similar to Fig. 4. Are highlighted in colors the Cretaceous-Paleogene age distribution from the middle Eocene CMB compilation (in purple) and Xigaze compilation (in green), and the age window of north Indian continental rifting (in red; van Hinsbergen et al., 2012), the Triassic-Jurassic age distribution from IBR Triassic-Lower Jurassic rocks (in purple) and the Xigaze compilation (in green), and the pre-400 Ma age distribution of the basement compilations from Fig. 4 for the Xigaze Basin (in green), IBR pre-Cretaceous rocks (in purple), and continental India (in red).

Fig. 6. Histograms and kernel density estimate diagrams for the **(a)** eastern and **(b)** central Himalayan Foreland Basin (HFB), and **(c)** The Tethyan Himalayan Sedimentary Series. Color coding and legend similar to Fig. 4.

4.3. Burma Terrane Accretionary Wedge (BTAW)

Age compilations from the BTAW are overall very similar to those from the CMB (Fig. 5b). They display the same PanaGren duo and a well-marked Triassic population. The Eocene Phopkhur Formation of northern BTAW (Naga Hills) is devoid of Upper Cretaceous ages, but more southerly units from the Chin Hills and the Arakan Yoma are dominated by Upper Cretaceous-Cenozoic ages, with similar age peaks and chronological evolution to what is observed in the CMB. We note the absence of a well-defined Jurassic population, but most BTAW compilations contain only a few pre-Cretaceous zircons, making it difficult to draw definitive conclusions about its presence.

4.4. Bengal and Assam Basins (BAB)

All age compilations from the BAB are dominated by Precambrian-Cambrian ages, except for the middle Eocene, where Upper Cretaceous-Paleogene ages make a significant contribution (Fig. 5c). They all display a well-marked PanaGren duo and an Eburnean (1600–1900 Ma) population, except during the middle Eocene, where the Eburnean population is nearly absent. The Panafrican population contributes equally to the other Precambrian populations during the Paleocene-early Eocene and late Eocene-Oligocene periods; it becomes prominent during the middle Eocene and Miocene.

All age compilations show a few Triassic ages, but their number is insufficient to confirm the presence and age of a distinct Triassic peak. They also all exhibit a continuous population of Upper Cretaceous-Paleogene ages. The amount is only sufficiently high in the middle Eocene compilation, where the age distribution is intermediate between those of the CMB and the Xigaze Basin, featuring a clear peak centered at 90 Ma, fewer younger grains, and a secondary population around 70 Ma.

4.5. Eastern Himalayan Foreland Basin (HFB)

The Paleocene-lower Eocene compilation of the eastern HFB is almost completely devoid of post-Panafrican zircons (Fig. 6a). It displays a continuous population of Precambrian to Cambrian zircons, with Panafrican, Grenvillian, and Eburnean populations in similar proportions, and a minor Liberian (2400–2600 Ma) population. The middle Eocene compilation, though consisting of a low number of zircons ($n < 500$), shows a distinct distribution with small but clear Upper Cretaceous and Triassic age populations, as well as a prominent PanaGren

Duo. The Miocene age compilation reveals a continuous Upper Cretaceous-Cenozoic age population with two age peaks centered at 50 and 90 Ma, a prominent Panafrican population, and two secondary Grenvillian and Eburnean populations that resemble the Miocene age compilation of the BAB (Fig. 5c).

4.6. Central Himalayan Foreland Basin (central HFB)

Cretaceous-lower Paleocene samples from the central HFB are devoid of Upper Cretaceous-Paleocene ages but exhibit a well-marked early Cretaceous (110–125 Ma) age population (Fig. 6b). They do not show the PanaGren Duo, unlike most compilations investigated here, but do feature well-marked Eburnean (1800–2000 Ma) and Liberian (2400–2600 Ma) populations. The middle Eocene and Miocene age compilations from the central HFB are distinct from both the Cretaceous-lower Paleocene compilation and the contemporaneous samples from the eastern HFB. The middle Eocene central HFB compilation is nearly devoid of Upper Cretaceous-Cenozoic grains but still displays an early Cretaceous population. It features a well-marked Permian-Triassic age population and a continuous population of Precambrian to Cambrian zircons, with an unusually small population of Panafrican ages. The Miocene compilation reveals the same continuous population of Precambrian to Cambrian zircons; post-Panafrican ages are nearly absent, with only a few grains centered around 90 Ma.

4.7. The Tethyan Himalayan Series (THS)

Cretaceous-lower Paleocene THS samples display a well-marked late Jurassic-early Cretaceous (115–150 Ma) age population (Fig. 6c). They also exhibit the same PanaGren duo found in most compilations. Upper Cretaceous grains are completely absent. The Paleocene-lower Eocene THS compilation shows an age distribution that closely resembles that of the Xigaze Basin. Post-Panafrican ages are prominent, displaying similar Jurassic to Paleogene populations with peaks centered around 90 Ma and 60 Ma. There is a notable widening of the Jurassic population towards late Triassic times (140–210 Ma). The PanaGren Duo is prominent in Precambrian-Cambrian ages and is found in similar proportions as in the Xigaze Basin.

5. Discussion

5.1. Signature zircon populations of Burmese, Asian, and Indian margin provenance

The PanaGren duo is ubiquitous in the samples of our regional database and reflects the shared early Gondwanan history of the Indian continent and the Lhasa and Burma Terranes. Consequently, Precambrian-Cambrian age populations are difficult to use for distinguishing the age distributions of potential source areas (Fig. 4). The overwhelming presence of the PanaGren duo in Precambrian-Cambrian zircon ages is only absent in the continental India compilation, where Eburnean (1800–2000 Ma) and Liberian (2400–2600 Ma) age populations are more significant (Fig. 4). Precambrian units, including multiple lower Proterozoic units, constitute most of the exposure of continental India, which likely explains why older ages are more prominent there. The strong expression of Eburnean and Liberian age populations is also observed in the Cretaceous-lower Paleocene pre-collisional units of the central HFB (Fig. 6a), and is interpreted as sourced from continental India (DeCelles et al., 2014). Paleozoic and Proterozoic units of the THS, Greater Himalaya, and Lesser Himalayas also display age distributions where Eburnean (1800–2000 Ma) and Liberian (2400–2600 Ma) age populations are prominent (Gehrels et al., 2011), although this is not the case in Cretaceous-lower Paleocene THS sedimentary rocks (Fig. 6c). Their very limited presence in late Mesozoic-lower Paleocene THS sediment suggests that the Cretaceous-lower Paleocene THS were not directly sourced from the continental Indian basement but rather locally sourced on the Greater Indian margin, from the recycling of younger units of its sedimentary cover. Therefore, a marked proportion of Eburnean and Liberian age populations can be considered a signature of the erosion of either continental India or deep units of the Himalayas.

The well-marked Triassic population found in Burma Terrane basement rocks, in the CMB, and in the BTAW is absent in Lhasa-derived Xigaze Basin sediment and in the pre-Cretaceous compilation of the Indian continent (Fig. 4). However, it is identical to the population found in the Langxijie Group of the eastern THS (Liu et al., 2020). The presence of this population in our basin compilations could thus alternatively reflect an input from the Burma Terrane basement or from the exhumation and erosion of the THS in the eastern Himalayan syntaxis. We note that Katha-Gangaw rocks also share a wide Triassic population; we therefore suggest that the Burma Terrane, Katha-Gangaw Range, and Langxijie Group share a similar origin (Yao et al., 2017; Liu et al., 2020).

Xigaze Basin rocks display a continuous record of ages from the Jurassic to the Eocene, with two prominent populations centered around 155 Ma and 90 Ma, and a minor population at 60 Ma. While the latter two are shared with the WPA in the CMB, the 155 Ma age population is unique to the Xigaze Basin. The 155 Ma event corresponds to a trench retreat, ophiolite spreading, and a magmatic flare-up episode along the Lhasa margin (Kapp and DeCelles, 2019). During this episode, Gangdese magmatism would have moved southward onto a forearc ophiolite, forming the short-lived Jurassic Zedong Arc (Metcalf and Kapp, 2019). This population is also found in Kohistan plutons at the western edge of the India-Asia collision zone, marking the onset of Kohistan magmatism (Jagoutz et al., 2019). There is evidence for 170–150 Ma oceanic spreading in Myanmar (e.g., Yui et al., 2013), but WPA magmatic activity does not commence before 130 Ma and has not left any earlier felsic, zircon-yielding batholith (Licht et al., 2020). This age population is absent in WPA plutons, as well as in Cretaceous and Paleocene-lower Eocene sediments of the CMB and the BTAW (Fig. 5a and 5b). Instead, CMB and BTAW rocks display the trio of 50, 70, and 95 Ma ages identified by Bandopadhyay et al. (2022).

Finally, the early Cretaceous (115–140 Ma) population found in Cretaceous-lower Paleocene THS and HFB sediments corresponds to the age of the intracontinental rifting episode of northern India (van Hinsbergen et al., 2012) and volcanic deposits found locally on the Indian continent (Baral et al., 2022).

A synthesis of these fingerprinting zircon age populations is provided in Table 1 and will be used in the forthcoming sections.

5.2. The Paleocene collision record in the HFB: Input from the Xigaze Forearc or an alternate arc?

As previously noted by studies such as Orme et al. (2015), the age distribution of Paleocene-lower Eocene post-collisional THS rocks shows the same Triassic to Cenozoic age populations as Xigaze Basin material (Fig. 6c), as well as the PanaGren duo common to most regional terranes. This similarity has been used to argue for a direct input of sediment from

Table 1
Main zircon populations observed in our compilations.

Fingerprinting zircon populations	areas
PanaGren duo: Panafrican (500–700 Ma), Grenvillian (800–1300 Ma)	All areas considered
Eburnean (1800–2000 Ma) and Liberian (2400–2600 Ma)	Continental India, Proterozoic-Paleozoic units of the Himalayas (Gehrels et al. (2011)
Permian-Triassic (280–210 Ma)	All Burma Terrane rocks, Katha Gangaw Range and eastern THS (Langxijie Group)
Jurassic (150–170 Ma)	Xigaze forearc (& Kohistan Arc; Jagoutz et al., 2019)
Lower Cretaceous (115–140 Ma)	Continental India (Intracontinental rifting episode)
Upper Cretaceous – Paleogene Burmese trio (50, 70 and 95 Ma)	Burma Terrane sedimentary basins

the Asian Gangdese Arc into the Tethyan Himalayas via the Xigaze Basin (Fig. 1a and 1b; Orme et al., 2015). It has also been interpreted as reflecting an input from an offshore Xigaze Forearc belonging to the Trans-Tethyan Arc (Fig. 1c; Kapp and DeCelles, 2019). In contrast, Trans-Tethyan models that do not include the Xigaze Forearc argue that these Triassic to Cenozoic age populations could alternatively reflect an allochthonous input from another hypothetical arc located between the Xigaze Forearc and India (Jagoutz et al., 2019; Westerweel et al., 2024).

To test this alternative scenario, we use our mixture modeling approach on the Paleocene-lower Eocene THS compilation (Fig. 7a). We distinguish the contribution of three sources: (1) the Greater India margin, represented by the Cretaceous-lower Paleocene pre-collisional THS compilation; (2) the Xigaze Forearc, represented by the Xigaze Basin age compilation; (3) an alternative arc, arbitrarily represented here by the Paleocene-lower Eocene CMB compilation, as the Burma Terrane is the only other proposed relic of the Trans-Tethyan Arc in the eastern sector of the collision zone (Westerweel et al., 2019; 2020). Our modeling approach is used on the younger part (ages < 400 Ma) of the compilations because the three potential sources do not display any significant difference in older age populations; additionally, adding these older populations to the modeling would result in an unsolvable mixture, as the source compilations display a much smaller amount of older ages than the THS compilations. Our modeling shows that a simple mixture composed of 80 % contribution from the Xigaze Forearc and 20 % from the Indian margin can statistically reproduce the Triassic to Cenozoic ages found in the Paleocene-lower Eocene THS compilation. These results are independent of the compilation chosen to represent the alternative arc: an alternative contribution is not necessary to statistically fit the THS post-collisional compilation. It also indicates that these ages can be partly explained by a mixture of input from the Burma Terrane and the Indian margin. However, this mixture alone is insufficient and always requires some contribution (>30 %) from the Xigaze Forearc to perfectly match the Triassic to Cenozoic ages in the Paleocene-lower Eocene THS compilation. Using the Xigaze Basin compilation restricted to Paleocene-Eocene ages instead of the complete compilation yields similar results (not shown).

The input of allochthonous material into the THS starting in the Paleocene is thus best explained by some contribution from the Xigaze Forearc. Our modeling confirms that the 61–59 Ma allochthonous input reflects incipient collision with the Xigaze Forearc, either along the Lhasa Terrane (Wu et al., 2014; Hu et al., 2015) or hundreds of kilometers away from it (Kapp and DeCelles, 2019). Although our modeling does not reject the possibility of a partial contribution from another arc, this hypothetical arc would have had to be either accreted or located adjacent to the Xigaze Forearc to explain the mandatory Xigaze-derived input in all best-fit mixtures.

5.3. Deciphering later collisional records in the HFB and BAB

In the eastern HFB and BAB, coeval Paleocene-lower Eocene deposits do not exhibit any clear input from the Xigaze Forearc or the Burma Terrane. Both regions show Eburnean and Liberian populations that are not obscured by an overwhelming PanaGren duo, indicating a predominant influence from continental India (Table 1). However, the BAB compilation does include a minor Cenozoic grain population as well as some Triassic grains, though their low abundance precludes conclusive provenance testing via mixture modeling.

The first significant post-Panafrican age population in the HFB and BAB emerges in the Middle Eocene BAB compilation. Middle Eocene BAB samples are notably devoid of Permian to Jurassic ages that might be associated with the Burma Terrane or the Xigaze Forearc. Instead, they display a well-defined Cretaceous-Cenozoic age population, with a prominent peak at 90 Ma. Ding et al. (2022) proposed that this population represents a mixture of both WPA and Gangdese Arc sources and implies an initial input of Burma Terrane sediment onto the Indian shelf. To determine which Cretaceous-Cenozoic Arc is the primary contributor to these ages, we employ the same mixture modeling approach (Fig. 7b). We consider three sources: (1) the Xigaze Forearc (represented by the

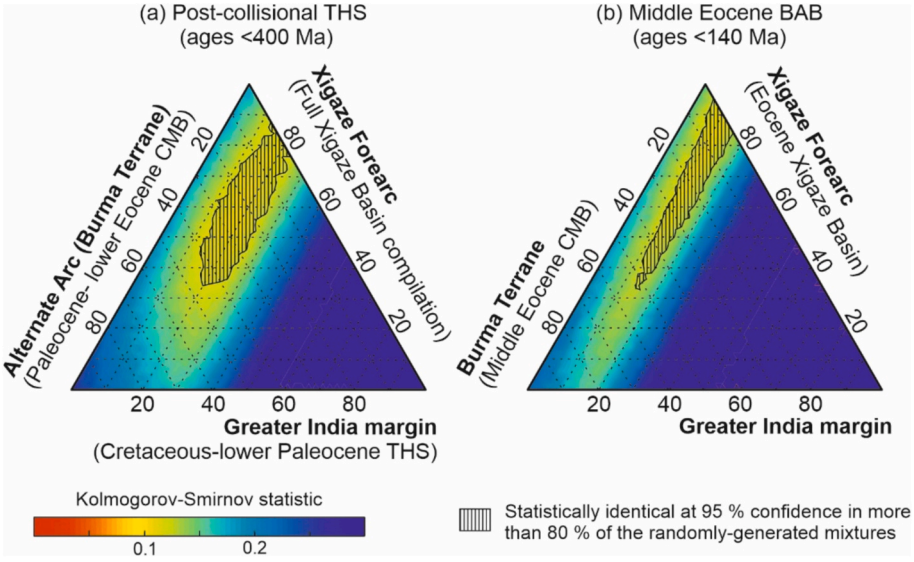

Fig. 7. (a) Dissimilarity to the post-collisional, Paleocene-Eocene THS age compilation for each possible combination of three potential source regions (The Xigaze Forearc, represented by the Xigaze Basin compilation; the Greater India margin, represented by the pre-collisional, Cretaceous-lower Paleocene THS age compilation; and an alternate arc, represented arbitrarily by the Paleocene-lower Eocene CMB compilation). Ages older than 400 Ma were excluded from the compilations. **(b)** Dissimilarity to the Middle Eocene BAB age compilation for each possible combination of three potential source regions (the Burma Terrane, represented by the middle Eocene CMB compilation; the Xigaze Forearc; represented by the Xigaze Basin compilation restricted to its Eocene samples; and the Greater India margin, represented by the same age compilation as for Fig. 7a). Ages older than 140 Ma were excluded from the compilations. The color bar indicates the range of values for the dissimilarity measure, here the Kolmogorov-Smirnov (KS) statistic averaged for N random synthetic distributions per source combination (N = 200). The combinations that best fit the tested compilation (post-collisional THS or middle Eocene BAB) are the ones that give the lowest dissimilarity values. An alternative way to determine the best fit is to look at the range of combinations for which more than 80 % of the N random synthetic distributions are statistically similar to the tested compilation (here in the sense of the KS statistic at the 95 % confidence level; zone filled with vertical lines).

Xigaze Basin compilation restricted to its Eocene samples, as Eocene ages are more prominent in this subset); (2) the Burma Terrane (represented by the middle Eocene CMB compilation); and (3) the Greater India margin. As previously, we apply the approach on the youngest part of the compilation, limited here to ages < 140 Ma instead of < 400 Ma, because of the low abundance of Triassic grains in the BAB compilation.

Similar to the post-collisional THS sedimentary budget, our modeling shows that a mixture consisting of 85 % contribution from the Xigaze Forearc and 15 % from the Indian margin can statistically reproduce the Cretaceous to Cenozoic ages observed in the middle Eocene BAB compilation. These ages can also be accounted for by an alternative triple mixture of Burma Terrane, Xigaze Forearc, and Indian inputs; however, a contribution from the Burma Terrane is not necessary to explain the age distribution of middle Eocene BAB sediment.

Thus, there is currently no statistical requirement for a significant input from the Burma Terrane into the BAB during the middle Eocene, nor in earlier times. Although our modeling does not exclude a minor contribution from the Burma Terrane during the middle Eocene (<50 %; Fig. 7b), it should be relatively small if present. The significant contribution of upper Cretaceous-Cenozoic ages to the BAB is notably absent in the upper Eocene-Oligocene (Barail Formation; Fig. 3). The base of the Barail Formation, dated at approximately 38 Ma (Najman et al., 2008), coincides with a major uplift event in the IBR, which corresponds to the deposition of the Phokphur Formation and the final emergence of the BTAW in the central segment of the IBR (Chin Hills; Licht et al., 2019; Aitchison et al., 2019). This synchronicity suggests that the reduction in Cretaceous-Cenozoic ages in the BAB compilation may result from the loss of a sediment routing system between central Myanmar and the BAB.

The subsequent reappearance of a significant upper Cretaceous-Cenozoic age population in the Miocene eastern HFB and the convergence of age distributions in the Miocene eastern HFB and BAB have been interpreted as indicating the establishment of an integrated Brahmaputra-Tsangpo drainage system, transporting young zircons of Gangdese Arc origin to the Indian shelf (Lang and Huntington, 2014). While a potential contribution from the Burma Terrane cannot be entirely ruled out, given the relatively high Miocene exhumation rates of the BTAW (Najman et al., 2022), it remains less certain.

5.4. First record of Asia-derived sediment on the Burma Terrane

The age compilations from the CMB and BTAW exhibit consistent PanaGren duo, Triassic, and upper Cretaceous–Cenozoic age populations. Notably, a minor Jurassic age population (140–180 Ma), similar to that observed in the Xigaze Basin (Table 1), appears in the middle Eocene and subsequent compilations but is absent in the Paleocene-lower Eocene compilation. To assess the statistical significance of this new population, we applied our mixture modeling approach to the CMB and BTAW compilations (Fig. 8). This analysis focuses on ages > 140 Ma to avoid biases introduced by younger ages, which are significantly influenced by coeval magmatic rocks from the WPA of the Burma Terrane. We distinguished contributions from three sources: the Xigaze Forearc (represented by the Xigaze Basin compilation), the IBR Triassic-lower Jurassic basement, and the Katha-Gangaw Range, all depicted in their respective age compilations from Fig. 4. Restricting the Xigaze Basin compilation to Paleocene-Eocene or Eocene-only ages instead of using the complete dataset yields similar results, as they display the same pre-140 Ma age populations (not shown).

Our modeling indicates that the Paleocene-lower Eocene and Miocene CMB age compilations, as well as the Eocene BTAW age compilation, can be explained by a predominant contribution from the IBR pre-Cretaceous basement, although a minor contribution from the other two sources is not excluded (Fig. 8a, 8b, and 8e). The Middle Eocene compilation cannot be solely explained by an input from the IBR pre-Cretaceous basement and requires an additional contribution from zircons with a Xigaze Forearc signature and/or from the Katha-Gangaw Range (Fig. 8b). The Oligocene compilation necessitates a combination of contributions from the IBR pre-Cretaceous basement and the Xigaze Forearc, with the best fit achieved by a 70 % contribution from the IBR basement and a 30 % contribution from the Xigaze Forearc (Fig. 8c).

The Oligocene is therefore the first time window for which a statistically significant allochthonous input into the CMB is required to explain the age distribution. This Xigaze Forearc signature could reflect the development of an Oligocene drainage system parallel to the Indus-Tsangpo suture zone, transporting Xigaze material into the CMB (Robinson et al., 2014; Westerweel et al., 2024). Alternatively, it could indicate direct input from the Asian margin, particularly the Asian Sibumasu margin (the MMMB; Fig. 2b), where 170 Ma plutons are prevalent (Licht et al., 2020).

This Oligocene age is consistent with rutile U-Pb ages from the CMB, which suggest the emergence of a new age population attributed to the Asian margin in the early Oligocene (Najman et al., 2022). This shift may have occurred as early as the late Eocene, given that no upper Eocene units have been sampled for rutile and zircon geochronology thus far (see Fig. 3). The requirement for an input from the Katha-Gangaw Range and/or the Xigaze Forearc/Asian margin in the middle Eocene suggests a potential collision between Asia and the Burma Terrane as early as the middle Eocene. However, further investigation is needed to confirm the Lhasa or Burma Terrane affinity of the Katha-Gangaw Range.

Finally, our modeling results do not statistically necessitate a

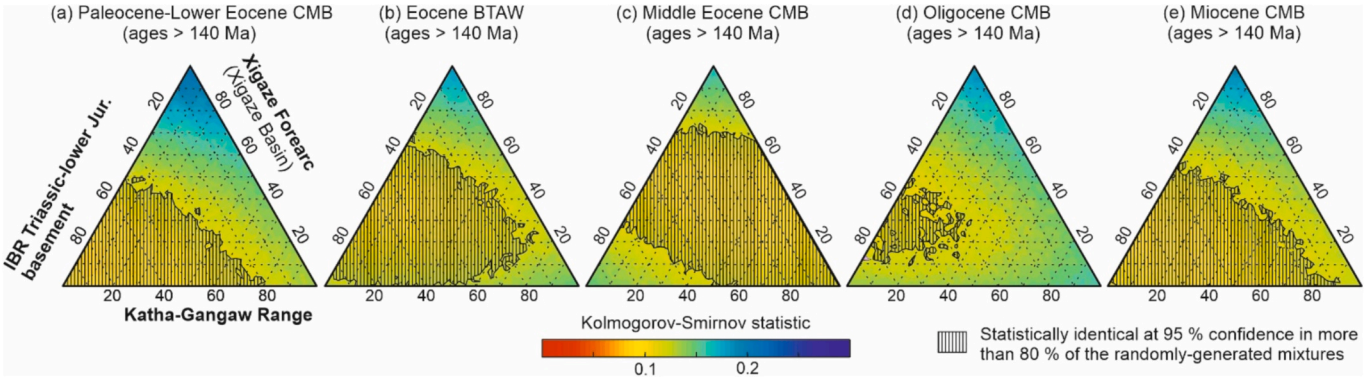

Fig. 8. Dissimilarity to (a) Paleocene – lower Eocene CMB, (b) Eocene BTAW (excluding the Phokphur Formation), (c) Middle Eocene CMB, (d) Oligocene and (e) Miocene CMB age compilation for each possible combination of three potential
Source regions (the IBR Triassic-lower Jurassic basement, the Katha-Gangaw Range, and the Xigaze Forearc). Ages younger than 400 Ma were excluded from the compilations. Legend: see Fig. 7.

significant Asian input to explain the Miocene CMB age distribution. Nonetheless, the bimodal distribution of Cenozoic ages in the Miocene CMB compilation resembles that observed in the BAB and eastern HFB for contemporaneous depositional ages, suggesting an input from Lhasa-derived volcanism, likely sourced from the MMMB and/or the eastern Himalayan Syntaxis (Westerweel et al., 2020).

5.5. Implications for Trans-Tethyan India-Asia collision models

Our analysis demonstrates that there is no statistical support in our high-resolution detrital zircon compilations for a Paleocene collision between India and a Trans-Tethyan Arc that excludes the Xigaze Forearc. The allochthonous material reaching the Tethyan Himalayas (THS) in the late Paleocene can be fully accounted for by a sole input from the Xigaze Forearc. While a contribution from the (Greater) Burma Terrane could partly explain this input, it still requires a significant contribution from the Xigaze Forearc. These results thus refute Trans-Tethyan geodynamic models for the India-Asia collision that do not incorporate the Xigaze Forearc as part of the Trans-Tethyan Arc (Fig. 1c; Jagoutz et al., 2019; Westerweel et al., 2024).

To align with the provenance constraints provided here and the paleomagnetic data from Myanmar (Westerweel et al., 2019), Trans-Tethyan models must include a composite Trans-Tethyan Arc incorporating both the Xigaze Forearc and the Burma Terrane. For this composite Xigaze-Burma Terrane Trans-Tethyan model, the first clear input of allochthonous material into the CMB, dated here and elsewhere (Najman et al., 2022) to the Oligocene, offers a possible chronological constraint for the docking of the India-Trans-Tethyan Arc assemblage to Asia. Alternatively, the Oligocene arrival of allochthonous material in the CMB could be attributed to the central Xigaze segment of the Trans-Tethyan Arc. An earlier, middle Eocene input of allochthonous material is also recorded in the CMB, although its origin remains uncertain.

A synchronous late Jurassic or early Cretaceous separation from the Asian margin for both terranes is currently the simplest model for the origin of this composite arc (Fig. 9a; Zahirovic et al., 2016). However, this scenario presents several issues. The Gondwana affinity of Cretaceous fossils from the Burma Terrane (e.g., Wood and Wunderlich, 2023) and the Gondwana-derived Pre-Cretaceous rocks in the BTAW (Yao et al., 2017) have been used to argue against an Asian origin for the Burma Terrane (Westerweel et al., 2024). These affinities could be explained by the accretion of Argoland fragments to this arc during the early Cretaceous (Morley et al., 2020). More problematically, the proposed timing for the separation of the Xigaze Forearc from the Lhasa margin is the late Cretaceous, associated with the Spong Volcanics of the Indus-Tsangpo Suture Zone (ca. 90 Ma; Kapp and DeCelles, 2019). A much earlier separation of the Xigaze Forearc would necessitate the existence of an active Xigaze Arc for at least 70 million years to supply the Xigaze Basin with Cretaceous to Paleogene zircons. The magmatic flare-up episodes of this arc would partially mimic those of the Gangdese Arc (Fig. 9b). Until further remnants of this Xigaze Arc are found along the Indus-Tsangpo Suture Zone, the Gangdese Arc remains the most plausible source of Xigaze Forearc zircons, which is inconsistent with an early separation of the Xigaze Forearc from the Asian margin.

One possible resolution to these issues is to consider a polygenetic nature for the Trans-Tethyan Arc, with a Xigaze Arc segment separating from Asia during the late Cretaceous, an earlier eastern segment comprising the Burma Terrane, and possibly other segments further west, such as the intra-oceanic Kohistan and Dras Arcs formed during the late Jurassic (Jagoutz et al., 2019; Andjić et al., 2022). This polygenetic Trans-Tethyan Arc would have been spatially discontinuous and would have straddled the Neotethys from west to east only during a brief time window (90–60 Ma). This scenario is compatible with paleomagnetic constraints for all these blocks (Westerweel et al., 2019; Martin et al., 2020; Xu et al., 2025). It would yet involve multiple crustal fragments and arc segments of varying origins, implying different episodes of subduction initiation and drifting spanning between the late

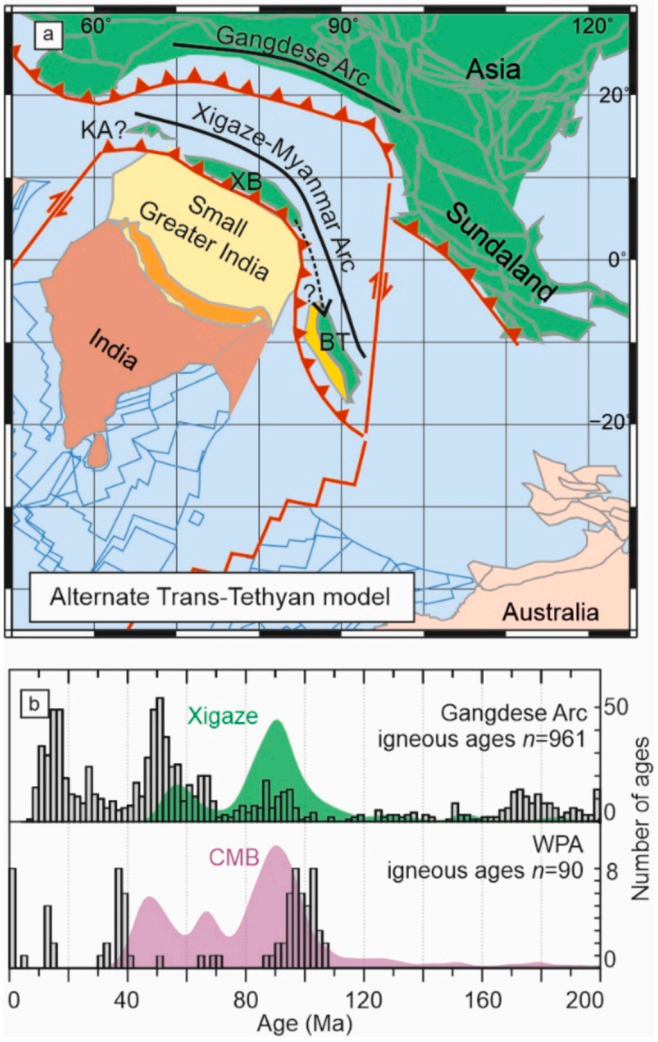

Fig. 9. (a) Plate reconstruction at ca. 60 Ma highlighting an alternate geodynamic model for the India-Asia collision with a Trans-Tethyan, Xigaze-Myanmar arc separated from Asia during the late Jurassic or early Cretaceous (Zahirovic et al., 2016). KA: Kohistan Arc; XB: Xigaze Basin; BT: Burma Terrane. Color coding similar to Fig. 1. The dashed arrow highlights the hypothetical drainage proposed by Westerweel et al. (2024) to explain late Cretaceous zircons in the CMB. (b) Crystallization age compilation from the WPA and the Gangdese Arc (compilations from Licht et al., 2020, including U-Pb, K-Ar and Ar-Ar igneous ages), compared to the kernel density estimate of the middle Eocene CMB zircon compilation (in purple) and the Xigaze Basin compilation (Eocene samples only; in green).

Jurassic and the mid Cretaceous, and a complex assemblage history during the middle to late Cretaceous. Such a scenario is thus challenging to visualize and remains to be clearly delineated. It would, however, be consistent with the current complexity of recent kinematic models for the Neotethys along its other sections, such as the Mediterranean domain (van Hinsbergen et al., 2020) and Southeast Asia (Advokaat and van Hinsbergen, 2024).

5.6. The missing arc of the Burma Terrane

While there is no statistical requirement for an unknown arc segment to explain the zircon populations in the Cenozoic Indian shelf basins and the Xigaze Forearc, the provenance of Cretaceous-Cenozoic zircons in the CMB is more complex. The primary zircon age populations found in the CMB do not align well with the geochronological compilations from Gangdese and WPA igneous rocks (Fig. 9b). WPA ages exhibit only two

prominent populations at approximately 100 and 40 Ma, and there are no known igneous rocks of 50 and 70 Ma age on the Burma Terrane (Licht et al., 2020). To address this discrepancy, Westerweel et al. (2024) proposed that a paleo-drainage along the Trans-Tethyan Arc might have transported volcanic material into the CMB (Fig. 9a).

In the context of a composite Xigaze-Burma Terrane Trans-Tethyan model, our mixture modeling does not exclude a potential Xigaze-CMB connection, as a minor contribution from the Xigaze Forearc is statistically plausible as early as the Cretaceous CMB compilation (Fig. 8). However, the formation of such a drainage seems unlikely before the Paleocene collision between India and the Trans-Tethyan Arc, as there would have been no significant topography or morphological barrier to facilitate sediment transport axially along the arc. Consequently, this scenario alone cannot account for the prominent 70 Ma age population observed in the Cretaceous CMB. Additionally, paleocurrent, isotopic, and petrographic data from the Eocene CMB do not support the existence of a long-distance drainage and instead suggest a local origin for the CMB material (Licht et al., 2013).

Following Bandopadhyay et al. (2022), we propose that the current magmatic rocks of the WPA in Myanmar are remnants of an arc with a much longer history of activity. These remnants were likely preserved due to their proximity to the ancient trench, whereas other rocks of the WPA were situated further east of the Burma Terrane. These rocks may have been lost through subduction or left behind as slivers along the Asian margin in Sibumasu. In this regard, the 100 and 40 Ma WPA plutons possibly reflect the trench-ward migration of the arc and slab rollback episodes along the Burmese subduction margin. Hafnium data from the prominent 70 Ma detrital zircon age population in the CMB support an origin from a broader WPA, as they exhibit εHf values similar to those found in 40 Myr and 100 Myr old igneous rocks in the modern WPA (Wang et al., 2014; Zhang et al., 2017). This suggests a comparable juvenile magma source. The origin and history of the Burma Terrane arc remain yet to be fully elucidated, and its relics should be carefully sought in Southeast Asia.

5.7. *Greater India models: Simpler alternatives?*

A collision at 61–59 Ma with the Xigaze Forearc is compatible with current Greater India models (e.g. Fig. 1a & b). Detrital zircon age compilations fail providing a clear age constraint for the docking of the eastern edge of India with the Burma Terrane, limiting their relevance for testing these models in the context of the Greater India – Burma Terrane collision chronology. Cenozoic zircons in the BAB suggest a potential India- Burma Terrane collision as early as the Paleocene-early Eocene, though a later collision age cannot be ruled out. This Paleocene – early Eocene age is consistent with the chronology of ophiolitic thrusting onto the Indian shelf in the Naga Hills of the BTAW (Aitchison et al., 2019), but remains to be confirmed with more detrital zircon data. We note yet that Greater India models must account for the early Paleogene paleogeographic isolation of the Burma Terrane as indicated by paleomagnetic data (Westerweel et al., 2024), as well as for a drainage connection between the Burma Terrane and Asia starting at least during the early Oligocene, and possibly earlier in the Eocene, based on our results.

The kinematic model proposed by Advokaat and van Hinsbergen (2024), which is based on the Greater India oceanic basin model (Fig. 1b), is currently the only model consistent with these constraints. It suggests a Paleocene collision between the Himalayas and the Xigaze Forearc/Lhasa margin, followed by an early Eocene collision of the eastern tip of continental India with the Burma Terrane, and subsequent accretion of the Burma Terrane to Asia in the late middle Eocene.

Two additional points supporting the Greater India oceanic basin model are worth noting. The significant difference between the THS and HFB zircon age compilations during the Cretaceous (Fig. 6) indicates the presence of a pre-collisional divide north and south of the Himalayas, between the northernmost tip of Greater India and the more southerly parts of the Indian shelf. This observation does not constrain the crustal nature of Greater India but is consistent with a thicker, continental block at the northern tip of Greater India, in agreement with the Greater India oceanic basin model (van Hinsbergen et al.; 2012). Additionally, the late Cretaceous unconformity observed in the BTAW and the CMB (e.g., Fig. 3), whose origin remains unexplained, could reflect the transit of this continental block offshore the Burma Terrane, close to the BTAW. Nonetheless, Greater India models fail addressing and explaining the correlation between BTAW ophiolites and the Indus-Tsangpo Suture Zone, based on their spreading ages and mechanisms (e.g. Morley et al., 2020), and the similar, age, origin and early history for the Xigaze Forearc and the CMB (Cai et al., 2020). Moreover, the position of the BT on the Australian Plate within the Greater India oceanic basin model (Advokaat and Van Hinsbergen, 2024) is difficult to reconcile with paleomagnetic and geological constraints suggesting a similar motion and a close correlation of the BT with India over the Cenozoic (Morley et al., 2020; Westerweel et al., 2024).

6. Conclusion

Our dataset and statistical analyses demonstrate that the Paleocene input of allochthonous zircons onto the Indian shelf is most straightforwardly explained by a direct contribution from the Xigaze Forearc. We find no definitive evidence of Burma Terrane-derived zircons in Paleogene Indian shelf basins. While such an input could have commenced as early as the Paleocene to early Eocene, the current number of detrital zircon samples is insufficient to statistically test this hypothesis. The earliest recorded input of allochthonous zircons into Burmese sedimentary basins dates to the middle Eocene, although their precise origin remains unclear. The Oligocene zircon compilation from the CMB shows a clear contribution from Asia-derived zircons, consistent with the provenance of Oligocene rutile (Najman et al., 2022).

These geochronological constraints thus appear to contradict the latest Trans-Tethyan kinematic models (Westerweel et al., 2024). In contrast, the chronology of drainage connections aligns with the most recent kinematic reconstruction involving a Greater India oceanic basin (Advokaat and van Hinsbergen, 2024). Cretaceous age compilations from Indian basins also support the presence of a Himalaya continental block at the northern tip of India, forming a drainage divide. Greater India oceanic basin models, however, do not yet provide a comprehensive geological scenario for the India-Asia collision, as they fail to account for the similar tectono-magmatic histories observed in the Indus-Tsangpo Suture Zone, BTAW, CMB, and the Xigaze Basin, and a similar motion for India and the BT. Nevertheless, these models are currently the most compatible with the existing detrital zircon populations.

The only Trans-Tethyan model that aligns with current geological constraints involves a tectonic assemblage of the Burma Terrane, the Xigaze Forearc, and possibly other segments further west during the late Cretaceous. This polygenetic scenario would include multiple crustal fragments, subduction initiations, and arc segments of varying origins and remains to be fully delineated. Despite its potential complexity, it does not significantly differ from the complexity of kinematic models for other parts of the Neotethyan margin. The current disparity between the complexity of Southeast Asian kinematic models and the relatively simplified tectonic models for South Asia is pronounced. Understanding the India-Asia collision would benefit from considering it not merely as a continent–continent or continent-arc-continent collision but as a complex orogen involving multiple isolated arcs and continental fragments, which are still poorly defined and require further identification, study, and correlation.

Plain language summary

Sedimentary provenance studies indicate that the collision between the Indian and Asian continents occurred about 60 million years ago, based on the arrival of foreign sediments on the Indian shelf. To explain this early timing, geodynamic models propose that either India was

much larger before the collision or that India collided with another arc, known as the Trans-Tethyan Arc, which was situated between India and Asia and has since disappeared.

In this study, we analyzed a dataset of zircon minerals from sedimentary rocks around India, Myanmar, and Asia. Our goal was to determine if the ages of these zircons could help identify the origin of these sedimentary rocks and assess whether a missing arc played a role in the collision process.

Our analysis shows that the foreign material on India originated mainly from the Asian forearc and that there is no statistical support for a missing arc between India and Asia. However, the dataset suggests that the Burmese sedimentary record requires a missing arc between Myanmar and Asia. These results are compatible with current collision models involving a larger India, and place strict paleogeographic constraints on models involving a Trans-Tethyan Arc.

CRediT authorship contribution statement

Alexis Licht: Writing – review & editing, Writing – original draft, Visualization, Validation, Supervision, Software, Resources, Project administration, Methodology, Investigation, Funding acquisition, Formal analysis, Data curation, Conceptualization. **Guillaume Dupont-Nivet:** Writing – review & editing, Supervision, Funding acquisition. **Jan Westerweel:** Writing – review & editing, Investigation, Data curation. **Zaw Win:** Writing – review & editing, Investigation, Data curation. **Abel Guihou:** Writing – review & editing, Investigation, Data curation. **Pierre Deschamps:** Writing – review & editing, Investigation, Data curation. **Day Wa Aung:** Supervision, Project administration.

Declaration of competing interest

The authors declare that they have no known competing financial interests or personal relationships that could have appeared to influence the work reported in this paper.

Acknowledgments

This research was primarily funded by grants from the European Research Council (ERC) under the European Union's Horizon 2020 research and innovation program to AL (DISPERSAL, grant agreement No. 101043268) and GDN (MAGIC, grant agreement No. 649081). We thank Kyi Kyi Thein, Kyaing Sein, D. van Hinsbergen, M. Mueller, T. Ugrai, S. Shekut, A.-C. Brajon and the Alamanda Inn, J. Longerey, J. Dauvier, and P. Roperch for prolific discussions, and assistance in the field and in the lab.

Appendix A. Supplementary data

Supplementary data to this article can be found online at https://doi.org/10.1016/j.gr.2025.06.018.

References

Acharyya, S.K., 2007. Evolution of the Himalayan Paleogene foreland basin, influence of its litho-packet on the formation of thrust-related domes and windows in the Eastern Himalayas–A review. J. Asian Earth Sci. 31 (1), 1–17.

Advokaat, E.L., van Hinsbergen, D.J., 2024. Finding Argoland: Reconstructing a microcontinental archipelago from the SE asian accretionary orogen. Gondw. Res. 128, 161–263.

Alam, M., Alam, M.M., Curray, J.R., Chowdhury, M.L.R., Gani, M.R., 2003. An overview of the sedimentary geology of the Bengal Basin in relation to the regional tectonic framework and basin-fill history. Sed. Geol. 155 (3–4), 179–208.

Aitchison, J.C., Xia, X., Baxter, A.T., Ali, J.R., 2011. Detrital zircon U–Pb ages along the Yarlung-Tsangpo suture zone, Tibet: Implications for oblique convergence and collision between India and Asia. Gondw. Res. 20 (4), 691–709.

Aitchison, J.C., Ao, A., Bhowmik, S., Clarke, G.L., Ireland, T.R., Kachovich, S., Zhou, R., 2019. Tectonic evolution of the western margin of the Burma microplate based on new fossil and radiometric age constraints. Tectonics 38 (5), 1718–1741.

Andjić, G., Zhou, R., Jonell, T.N., Aitchison, J.C., 2022. A single Dras-Kohistan-Ladakh arc revealed by volcaniclastic records. Geochem. Geophys. Geosyst. 23 (3), e2021GC010042.

Bandopadhyay, P.C., van Hinsbergen, D.J., Bandyopadhyay, D., Licht, A., Advokaat, E.L., Plunder, A., Trabucho-Alexandre, J.P., 2022. Paleogeography of the West Burma Block and the eastern Neotethys Ocean: Constraints from Cenozoic sediments shed onto the Andaman-Nicobar ophiolites. Gondw. Res. 103, 335–361.

Baral, U., Lin, D., Goswami, T.K., Sarma, M., Qasim, M., Bezbaruah, D., 2019. Detrital zircon U–Pb geochronology of a Cenozoic foreland basin in Northeast India: Implications for zircon provenance during the collision of the Indian and asian plates. Terra Nova 31 (1), 18–27.

Baral, U., Ding, L., Goswami, T.K., Sarma, M., Jan, M.Q., Wang, C., Bezbaruah, D., 2022. Geochemical and geochronological studies of Abor volcanic rocks of eastern Himalaya. Geol. J. 57 (2), 482–502.

Bracciali, L., Najman, Y., Parrish, R.R., Akhter, S.H., Millar, I., 2015. The Brahmaputra tale of tectonics and erosion: Early Miocene river capture in the Eastern Himalaya. Earth Planet. Sci. Lett. 415, 25–37.

Cai, F., Ding, L., Zhang, Q., Orme, D.A., Wei, H., Li, J., Sein, K., 2020. Initiation and evolution of forearc basins in the Central Myanmar Depression. Bulletin 132 (5–6), 1066–1082.

DeCelles, P.G., Gehrels, G.E., Quade, J., Ojha, T.P., 1998. Eocene-early Miocene foreland basin development and the history of Himalayan thrusting, western and central Nepal. Tectonics 17 (5), 741–765.

DeCelles, P.G., Gehrels, G.E., Najman, Y., Martin, A.J., Carter, A., Garzanti, E., 2004. Detrital geochronology and geochemistry of Cretaceous–Early Miocene strata of Nepal: implications for timing and diachroneity of initial Himalayan orogenesis. Earth Planet. Sci. Lett. 227 (3–4), 313–330.

DeCelles, P.G., Kapp, P., Gehrels, G.E., Ding, L., 2014. Paleocene-Eocene foreland basin evolution in the Himalaya of southern Tibet and Nepal: Implications for the age of initial India-Asia collision. Tectonics 33 (5), 824–849.

Ding, L., Goswami, T.K., Cai, F.L., Baral, U., Sarmah, R.K., Bezbaruah, D., 2022. Detrital zircon U–Pb ages of Tertiary sequences (Palaeocene-Miocene): Inner Fold Belt and Belt of Schuppen, Indo-Myanmar Ranges. India. Geological Journal 57 (12), 5191–5206.

Feng, W., Meng, Q., Song, C., Fang, X., Zhuang, G., He, P., Zhang, Y., 2023. Constraints on the timing of the India-Asia collision and unroofing history of the Himalayan orogen using detrital zircon U-Pb-Hf and whole-rock Sr-Nd isotopes in Cretaceous-Miocene Lesser Himalayan sedimentary rocks. Basin Res. 35 (3), 949–977.

Garzanti, E., Hu, X., 2015. Latest cretaceous Himalayan tectonics: Obduction, collision or Deccan-related uplift? Gondw. Res. 28 (1), 165–178.

Gehrels, G., Kapp, P., DeCelles, P., Pullen, A., Blakey, R., Weislogel, A., Yin, A., 2011. Detrital zircon geochronology of pre-Tertiary strata in the Tibetan-Himalayan orogen. Tectonics 30 (5).

Govin, G., Najman, Y., Copley, A., Millar, I., Van der Beek, P., Huyghe, P., Davenport, J., 2018. Timing and mechanism of the rise of the Shillong Plateau in the Himalayan foreland. Geology 46 (3), 279–282.

van Hinsbergen, D.J., Kapp, P., Dupont-Nivet, G., Lippert, P.C., DeCelles, P.G., Torsvik, T. H., 2011. Restoration of Cenozoic deformation in Asia and the size of Greater India. Tectonics 30 (5).

van Hinsbergen, D.J., Lippert, P.C., Dupont-Nivet, G., McQuarrie, N., Doubrovine, P.V., Spakman, W., Torsvik, T.H., 2012. Greater India Basin hypothesis and a two-stage Cenozoic collision between India and Asia. Proc. Natl. Acad. Sci. 109 (20), 7659–7664.

Van Hinsbergen, D.J., Torsvik, T.H., Schmid, S.M., Maţenco, L.C., Maffione, M., Vissers, R.L., Spakman, W., 2020. Orogenic architecture of the Mediterranean region and kinematic reconstruction of its tectonic evolution since the Triassic. Gondw. Res. 81, 79–229.

Horstwood, M.S., Košler, J., Gehrels, G., Jackson, S.E., McLean, N.M., Paton, C., Schoene, B., 2016. Community-derived standards for LA-ICP-MS U-(Th-) Pb geochronology–uncertainty propagation, age interpretation and data reporting. Geostand. Geoanal. Res. 40 (3), 311–332.

Hu, X., Sinclair, H.D., Wang, J., Jiang, H., Wu, F., 2012. Late Cretaceous-Palaeogene stratigraphic and basin evolution in the Zhepure Mountain of southern Tibet: Implications for the timing of India-Asia initial collision. Basin Res. 24 (5), 520–543.

Hu, X., Garzanti, E., Moore, T., Raffi, I., 2015. Direct stratigraphic dating of India-Asia collision onset at the Selandian (middle Paleocene, 59±1 Ma). Geology 43 (10), 859–862.

Ingalls, M., Rowley, D.B., Currie, B., Colman, A.S., 2016. Large-scale subduction of continental crust implied by India–Asia mass-balance calculation. Nat. Geosci. 9 (11), 848–853.

Jagoutz, O., Royden, L., Holt, A.F., Becker, T.W., 2015. Anomalously fast convergence of India and Eurasia caused by double subduction. Nat. Geosci. 8 (6), 475–478.

Jagoutz, O., Bouilhol, P., Schaltegger, U., Müntener, O., 2019. The isotopic evolution of the Kohistan Ladakh arc from subduction initiation to continent arc collision. Geol. Soc. Lond. Spec. Publ. 483 (1), 165–182.

Jonell, T.N., Giosan, L., Clift, P.D., Carter, A., Bretschneider, L., Hathorne, E.C., Naing, T., 2022. No modern Irrawaddy River until the late Miocene-Pliocene. Earth Planet. Sci. Lett. 584, 117516.

Kapp, P., DeCelles, P.G., 2019. Mesozoic–Cenozoic geological evolution of the Himalayan-Tibetan orogen and working tectonic hypotheses. Am. J. Sci. 319 (3), 159–254.

Lang, K.A., Huntington, K.W., 2014. Antecedence of the Yarlung–Siang–Brahmaputra River, eastern Himalaya. Earth Planet. Sci. Lett. 397, 145–158.

Licht, A., France-Lanord, C., Reisberg, L., Fontaine, C., Soe, A.N., Jaeger, J.J., 2013. A palaeo Tibet–Myanmar connection? Reconstructing the late Eocene drainage

system of central Myanmar using a multi-proxy approach. J. Geol. Soc. London 170 (6), 929–939.
Licht, A., Pullen, A., Kapp, P., Abell, J., Giesler, N., 2016a. Eolian cannibalism: Reworked loess and fluvial sediment as the main sources of the Chinese Loess Plateau. Bulletin 128 (5–6), 944–956.
Licht, A., Dupont-Nivet, G., Pullen, A., Kapp, P., Abels, H.A., Lai, Z., Giesler, D., 2016b. Resilience of the asian atmospheric circulation shown by Paleogene dust provenance. Nat. Commun. 7 (1), 12390.
Licht, A., Dupont-Nivet, G., Win, Z., Swe, H.H., Kaythi, M., Roperch, P., Jones, D., 2019. Paleogene evolution of the Burmese forearc basin and implications for the history of India-Asia convergence. Bulletin 131 (5–6), 730–748.
Licht, A., Win, Z., Westerweel, J., Cogné, N., Morley, C.K., Chantraprasert, S., Dupont-Nivet, G., 2020. Magmatic history of central Myanmar and implications for the evolution of the Burma Terrane. Gondw. Res. 87, 303–319.
Licht, A., Folch, A., Sylvestre, F., Yacoub, A.N., Cogné, N., Abderamane, M., Deschamps, P., 2024. Provenance of aeolian sands from the southeastern Sahara from a detrital zircon perspective. Quat. Sci. Rev. 328, 108539.
Liu, Y.M., Dai, J.G., Wang, C.S., Li, H.A., Wang, Q., Zhang, L.L., 2020. Provenance and tectonic setting of Upper Triassic turbidites in the eastern Tethyan Himalaya: Implications for early-stage evolution of the Neo–Tethys. Earth Sci. Rev. 200, 103030.
Martin, C.R., Jagoutz, O., Upadhyay, R., Royden, L.H., Eddy, M.P., Bailey, E., Weiss, B.P., 2020. Paleocene latitude of the Kohistan–Ladakh arc indicates multistage India–Eurasia collision. Proc. Natl. Acad. Sci. 117 (47), 29487–29494.
Metcalf, K., Kapp, P., 2019. History of subduction erosion and accretion recorded in the Yarlung Suture Zone, southern Tibet. Geol. Soc. Lond. Spec. Publ. 483 (1), 517–554.
McNeil, J.D., Gough, A., Hall, R., Lünsdorf, N.K., Webb, M., Feil, S., 2021. A multi-proxy provenance study of Eocene to Oligocene sandstones in the Salin Sub-basin. Myanmar. Journal of Asian Earth Sciences 216, 104825.
Min, M., Ratschbacher, L., Franz, L., Hacker, B.R., Enkelmann, E., Toreno, E.Y., Pfänder, J.A., 2022. India (Tethyan Himalaya Series) in Central Myanmar: Implications for the Evolution of the Eastern Himalayan Syntaxis and the Sagaing Transform-Fault System. Geophys. Res. Lett. 49 (12), e2022GL099140.
Mitchell, A., 2017. *Geological belts, plate boundaries, and mineral deposits in Myanmar*. Elsevier.
Morley, C.K., Naing, T.T., Searle, M., Robinson, S.A., 2020. Structural and tectonic development of the Indo-Burma Ranges. Earth Sci. Rev. 102992.
Naing, T.T., Bussien, D.A., Winkler, W.H., Nold, M., Von Quadt, A., 2014. Provenance study on Eocene–Miocene sandstones of the Rakhine coastal belt, Indo-Burman Ranges of Myanmar: Geodynamic implications. Geol. Soc. Lond. Spec. Publ. 386 (1), 195–216.
Naing, T.T., Robinson, S.A., Searle, M.P., Morley, C.K., Millar, I., Green, O.R., Henderson, G.M., 2023. Age, depositional history and tectonics of the Indo-Myanmar Ranges, Myanmar. J. Geol. Soc. London 180 (5), jgs2022-091.
Najman, Y., Bickle, M., BouDagher-Fadel, M., Carter, A., Garzanti, E., Paul, M., Vezzoli, G., 2008. The Paleogene record of Himalayan erosion: Bengal Basin. Bangladesh. Earth and Planetary Science Letters 273 (1–2), 1–14.
Najman, Y., Sobel, E.R., Millar, I., Stockli, D.F., Govin, G., Lisker, F., Kahn, A., 2020. The exhumation of the Indo-Burman Ranges, Myanmar. Earth Planet. Sci. Lett. 530, 115948.
Najman, Y., Sobel, E.R., Millar, I., Luan, X., Zapata, S., Garzanti, E., Lwin, T.N., 2022. The timing of collision between Asia and the West Burma Terrane, and the development of the Indo-Burman Ranges. Tectonics 41 (7), e2021TC007057.
Orme, D.A., Carrapa, B., Kapp, P., 2015. Sedimentology, provenance and geochronology of the upper Cretaceous–lower Eocene western Xigaze forearc basin, southern Tibet. Basin Res. 27 (4), 387–411.
Pivnik, D.A., Nahm, J., Tucker, R.S., Smith, G.O., Nyein, K., Nyunt, M., Maung, P.H., 1998. Polyphase deformation in a fore-arc/back-arc basin, Salin subbasin, Myanmar (Burma). AAPG Bull. 82 (10), 1837–1856.
Puetz, S.J., Condie, K.C., 2019. Time series analysis of mantle cycles Part I: Periodicities and correlations among seven global isotopic databases. Geosci. Front. 10 (4), 1305–1326.
Pullen, A., Ibáñez-Mejía, M., Gehrels, G.E., Ibáñez-Mejía, J.C., Pecha, M., 2014. What happens when n= 1000? Creating large-n geochronological datasets with LA-ICP-MS for geologic investigations. J. Anal. At. Spectrom 29 (6), 971–980.
Rahman, M.J.J., Xiao, W., McCann, T., Songjian, A., 2017. Provenance of the Neogene Surma Group from the Chittagong Tripura Fold Belt, southeast Bengal Basin, Bangladesh: Constraints from whole-rock geochemistry and detrital zircon U-Pb ages. J. Asian Earth Sci. 148, 277–293.
Ravikant, V., Wu, F.Y., Ji, W.Q., 2011. U–Pb age and Hf isotopic constraints of detrital zircons from the Himalayan foreland Subathu sub-basin on the Tertiary palaeogeography of the Himalaya. Earth Planet. Sci. Lett. 304 (3–4), 356–368.
Robinson, R.A., Brezina, C.A., Parrish, R.R., Horstwood, M.S., Oo, N.W., Bird, M.I., Zaw, K., 2014. Large rivers and orogens: the evolution of the Yarlung Tsangpo–Irrawaddy system and the eastern Himalayan syntaxis. Gondw. Res. 26 (1), 112–121.
Shekut, S., Licht, A., 2020. Late middle Miocene emergence of the Olympic Peninsula shown by sedimentary provenance. Lithosphere 2020 (1), 7040598.
Vadlamani, R., Wu, F.Y., Ji, W.Q., 2015. Detrital zircon U–Pb age and Hf isotopic composition from foreland sediments of the Assam Basin, NE India: Constraints on sediment provenance and tectonics of the Eastern Himalaya. J. Asian Earth Sci. 111, 254–267.
Vermeesch, P., 2018. Dissimilarity measures in detrital geochronology. Earth Sci. Rev. 178, 310–321.
Vermeesch, P., 2021. On the treatment of discordant detrital zircon U–Pb data. Geochronology 3, 247–257.
Westerweel, J., Roperch, P., Licht, A., Dupont-Nivet, G., Win, Z., Poblete, F., Aung, D.W., 2019. Burma Terrane part of the Trans-Tethyan Arc during collision with India according to palaeomagnetic data. Nat. Geosci. 12 (10), 863–868.
Westerweel, J., Licht, A., Cogné, N., Roperch, P., Dupont-Nivet, G., Kay Thi, M., Wa Aung, D., 2020. Burma Terrane collision and northward indentation in the Eastern Himalayas recorded in the Eocene-Miocene Chindwin Basin (Myanmar). Tectonics 39 (10), e2020TC006413.
Westerweel, J., Roperch, P., Win, Z., Dupont-Nivet, G., 2024. Northward drift of the Burma Terrane with India during the Cenozoic and implications for the India-Asia collision. Geol. Soc. Lond. Spec. Publ. 549 (1), SP549-2024.
Wang, J.G., Wu, F.Y., Tan, X.C., Liu, C.Z., 2014. Magmatic evolution of the Western Myanmar Arc documented by U–Pb and Hf isotopes in detrital zircon. Tectonophysics 612, 97–105.
Wang, J.G., Hu, X., Garzanti, E., An, W., Liu, X.C., 2017. The birth of the Xigaze forearc basin in southern Tibet. Earth Planet. Sci. Lett. 465, 38–47.
Wood, H.M., Wunderlich, J., 2023. Burma terrane amber fauna shows connections to Gondwana and transported Gondwanan lineages to the northern hemisphere (Araneae: Palpimanoidea). Syst. Biol. 72 (6), 1233–1246.
Wu, F.Y., Ji, W.Q., Wang, J.G., Liu, C.Z., Chung, S.L., Clift, P.D., 2014. Zircon U–Pb and Hf isotopic constraints on the onset time of India-Asia collision. Am. J. Sci. 314 (2), 548–579.
Xu, S., Li, Y.X., van Hinsbergen, D.J., Liu, X., Li, B., Li, X., Wang, T., 2025. An asymmetric late cretaceous back-arc basin south of Tibet? Geology. https://doi.org/10.1130/G52634.1.
Yang, L., Xiao, W., Julleh Jalalur Rahman, M., Windley, B. F., Schulmann, K., Ao, S., ... & Li, R. (2019). Provenance of the C enozoic B engal B asin sediments: I nsights from U–P b ages and Hf isotopes of detrital zircons. Geological Journal, 54(2), 978-990.
Yao, W., Ding, L., Cai, F., Wang, H., Xu, Q., Zaw, T., 2017. Origin and tectonic evolution of upper Triassic Turbidites in the Indo-Burman ranges, West Myanmar. Tectonophysics 721, 90–105.
Yui, T.F., Fukoyama, M., Iizuka, Y., Wu, C.M., Wu, T.W., Liou, J.G., Grove, M., 2013. Is Myanmar jadeitite of Jurassic age? a result from incompletely recrystallized inherited zircon. Lithos 160, 268–282.
Zahirovic, S., Matthews, K.J., Flament, N., Müller, R.D., Hill, K.C., Seton, M., Gurnis, M., 2016. Tectonic evolution and deep mantle structure of the eastern Tethys since the latest Jurassic. Earth Sci. Rev. 162, 293–337.
Zhang, P., Mei, L., Hu, X., Li, R., Wu, L., Zhou, Z., Qiu, H., 2017. Structures, uplift, and magmatism of the Western Myanmar Arc: Constraints to mid-Cretaceous-Paleogene tectonic evolution of the western Myanmar continental margin. Gondw. Res. 52, 18–38.
Zhang, P., Najman, Y., Mei, L., Millar, I., Sobel, E.R., Carter, A., Hu, X., 2019. Palaeodrainage evolution of the large rivers of East Asia, and Himalayan-Tibet tectonics. Earth Sci. Rev. 192, 601–630.